PTEP

Prog. Theor. Exp. Phys. **2015**, 113B05 (35 pages)
DOI: 10.1093/ptep/ptv155

Signal of doubly charged Higgs at e^+e^- colliders

L. T. Hue[1,*], D. T. Huong[1], H. N. Long[1], H. T. Hung[2], and N. H. Thao[2]

[1] *Institute of Physics, Vietnam Academy of Science and Technology, 10 Dao Tan, Ba Dinh, 10000 Hanoi, Vietnam*
[2] *Department of Physics, Hanoi University of Education 2, Phuc Yen, 11000 Vinh Phuc, Vietnam*
*E-mail: lthue@iop.vast.ac.vn

Received April 6, 2015; Revised August 1, 2015; Accepted September 28, 2015; Published November 25, 2015

The masses and signals of the production of doubly charged Higgses (DCH) in the framework of the supersymmetric reduced minimal 3-3-1 model are investigated. In the DCH sector, we prove that there always exists a region of the parameter space where the mass of the lightest DCH is of the order of $\mathcal{O}(100)$ GeV even when all other new particles are very heavy. The lightest DCH mainly decays to two same-sign leptons while the dominant decay channels of the heavy DCHs are those decaying to heavy particles. We analyze each production cross section for $e^+e^- \to H^{++}H^{--}$ as a function of a few kinematic variables, which are useful to discuss the creation of DCHs in e^+e^- colliders as an indicator of new physics beyond the Standard Model. A numerical study shows that the cross sections for creating the lightest DCH can reach values of a few pb. The other two DCHs are too heavy, beyond the observable range of experiments. The lightest DCH may be detected by the International Linear Collider or the Compact Linear Collider by searching for its decay to a same-sign charged lepton pair.

Subject Index B12, B13, B53

1. Introduction

The detection of the Higgs boson, with a mass around 125 GeV, by experiments at the Large Hadron Collider (LHC) [1–4] has again confirmed the success of the Standard Model (SM). However, this model needs to be extended to cover other problems that cannot be explained in this framework, particularly small neutrino mass and mixing, dark matter (DM), asymmetry of matter and antimatter, etc. Theories that lie beyond the SM not only solve the SM problems but also predict the signals of new physics that can be searched for in the future. Many well known models beyond the SM have Higgs spectra containing doubly charged Higgses (DCHs), e.g., the left–right model [5–7], the Zee–Babu model [8,9], the 3-3-1 models [10–13], etc, and their supersymmetric versions [14–21]. The appearance of the DCHs will really be one of the signals of new physics. Hence, there have been a number of publications predicting this signal in colliders such as the LHC, International Linear Collider (ILC) [22,23], and Compact Linear Collider (CLIC) [24,25]. Recent experimental searches for the DCHs have been done at the LHC [26–29], through their decays into a pair of same-sign charged leptons. This decay channel has been investigated in many of the above models: the left–right symmetric model [30,31] and the supersymmetric version [32], and the 3-3-1 models [33,34]. On the other hand, some other SM extensions, including Higgs triplets, have shown that the DCHs may have main decay channels of $H^{\pm\pm} \to W^\pm W^\pm$ [35,36], or $H^\pm W^\pm$ [37], leading to lower bounds of DCH masses than those obtained by searching for DCH decay into leptons. It is noted that the Higgs

Funded by SCOAP[3]

sectors in the supersymmetric (SUSY) models seem to be very interesting because they do not contain unknown self-couplings of four Higgses in the superpotential, unlike the case of non-SUSY models, where these kinds of couplings directly contribute to the Higgs masses. As a consequence, some Higgses will get masses mainly from the D-term, namely, from the electroweak breaking scale, leading to values of Higgs masses being of the order of $\mathcal{O}(100)$ GeV at the tree level. This happens in SUSY models such as the minimal supersymmetric standard model (MSSM) and supersymmetric versions of the economical 3-3-1 (SUSYE331) and reduced minimal 3-3-1 (SUSYRM331) models [20,21,38]. It has been shown that there is at least one neutral CP-even Higgs inheriting a tree-level mass below the mass of the Z boson, $m_Z = 92$ GeV. Fortunately, the loop-correction contributions increase the full mass of this Higgs up to the recent experimental value. This suggests that some other Higgses may be light with masses of the order of $\mathcal{O}(100)$ GeV. In the MSSM, this cannot happen if soft parameters such as the b_μ term, related to the mass of the neutral CP-odd Higgs, are large. Other SUSY versions, such as the 3-3-1 models, are different because of the appearance of the $SU(3)_L$ scale apart from the SUSY scale. For SUSYE331, the parameters characterizing these two scales may cancel each other to create the light mass of the lightest singly charged Higgs [38]. In this work, we will investigate the DCHs in SUSYRM331 and prove that there may exist a light DCH, even if both the soft and $SU(3)_L$ parameters are very large. Apart from inheriting the lepton number two, this light DCH is also lighter than almost all of the new particles in the model, and therefore will decay mainly to a same-sign lepton pair. So the possibility of detection of the lightest DCH will increase at colliders such as the LHC, ILC, and CLIC. In the left–right symmetric model, the cross sections for DCH creation at the LHC are predicted below 5 fb for mass values greater than 200 GeV. In the SUSY left–right model, they are estimated below 10 fb with a collision energy of 14 TeV at LHC [30] and a DCH mass smaller than 450 GeV. The cross sections for the DCH creation will decrease if their masses increase. In the framework of the 3-3-1 model, the cross sections for creating DCHs can reach a value smaller than 10^2 fb in e^+e^- colliders [33,34]. Our work will concentrate on the signals of detecting DCHs at the ILC and CLIC because of their very high precision. In addition, the collision energies of the ILC and CLIC are smaller than that of the LHC but the total cross sections for creating DCHs at the ILC and CLIC are larger than those at the LHC.

Let us remind ourselves of the reason for studying 3-3-1 models. The 3-3-1 models not only contain the great success of the SM but can also solve many problems of the SM. In particular, the 3-3-1 models can provide small neutrino masses as well as candidates for the DM [39,40]. The decays of some new particles can solve the matter–antimatter asymmetry via leptogenesis mechanisms [41–43]. The 3-3-1 models can connect to the cosmological inflation [41–43]. In addition, the 3-3-1 models [10,11,13,44–49] have many intriguing properties. In order to make the models anomaly free, one of the quark families must transform under $SU(3)_L$ in a different way from the other two. This leads to a consequence that the number of fermion generations has to be a multiple of the color number, which is three. In combination with the QCD asymptotic freedom requiring the number of quark generations to be less than five, the solution is exactly three for the number of fermion generations required. Furthermore, the 3-3-1 models give a good explanation of the electric charge quantization [50–54].

It is to be noted that the unique disadvantage of the 3-3-1 models is the complication in the Higgs sector, which reduces their predictability. Recently, there have been some efforts to reduce the Higgs contents of the models. The first successful attempt was with the 3-3-1 model with right-handed neutrinos [44–49], giving a model with just two Higgs triplets. The model is called the economical

3-3-1 model [55–57]. A similar version to the minimal 3-3-1 model with a Higgs sector containing three triplets and one sextet is the reduced minimal 3-3-1 model with again just two Higgs triplets [12,58]. However, to give masses to all fermions in the 3-3-1 models with the minimal Higgs sector, one has to introduce effective couplings that are nonrenormalizable. On the other hand, by investigating the one-loop β-function in the minimal 3-3-1 model and its supersymmetric version, we can predict the existence of Landau poles that make these theories lose their perturbative character. In order to solve this problem, the cut-off $\Lambda \simeq \mathcal{O}(1)$ TeV should be implied [59,60]. For the nonsupersymmetric version, the upper bound of $\Lambda < 5$ TeV seems inconsistent with recent data from precision tests [61,62]. As a solution to this problem, the SUSY version predicts a less restrictive upper bound. Additionally, the ρ parameter, one of the most important parameters for checking the precision test at low energy [63,64], still satisfies the current data if SUSY contributions are considered [65]. In any case, discussions on the non-SUSY version predict that the valid scale of the SUSYRM331 should be large, resulting in very heavy masses for the new particles, except a light neutral CP-even Higgs and maybe the lightest DCH. Therefore, apart from the light neutral Higgs, which can be identified with the one observed at LHC recently, the lightest DCH is the only one that may be observed by recent experiments.

Once again, we would like to emphasize that the RM331 model contains the minimal number of Higgses; the first way to generate consistent masses for fermions is to introduce effective operators working at the TeV scale [21,66]. Besides that, in the SUSY versions the fermion masses can be generated by including radiative corrections through the mixing of fermions and their superpartners [20,67,68]. Of course, in this case, the well known R parity has to be broken. Based on these results, many supersymmetric versions have been built and studied, such as SUSYE331 [69–72], SUSYRM331 [20,21], etc. One of the intriguing features of supersymmetric theories is that the Higgs spectrum is quite constrained.

Our paper is organized as follows. In Sect. 2, we will briefly review the SUSYRM331 model, particularly concentrating on the Higgs and gauge boson sectors and their effect on the ρ parameter, which may indirectly affect the lower bound of the $SU(3)_L$ scale. Furthermore, some important and interesting properties of SUSYRM331 are discussed, e.g., (i) the soft and $SU(3)_L$ parameters should be of the same order; (ii) the model contains a light neutral CP-even Higgs with the values of the squared tree-level mass of $m_Z^2|\cos 2\gamma| + m_W^2 \times \mathcal{O}(\epsilon)$. Here γ is defined as the ratio of the two vacuum expectation values of two Higgses ρ and ρ', while ϵ is defined as a quantity characterizing the ratio of the electroweak and $SU(3)_L$ scales. Section 3 is devoted to investigating in detail the masses and other properties of the DCHs. We will discuss the constraint of the DCH masses under the recent experimental value of the decay of the lightest CP-even neutral Higgs to two photons. From this, we prove that there exists a region of parameter space containing a light DCH. In Sect. 4, we discuss the creation of DCHs in e^+e^- colliders such as the ILC and CLIC. Specifically, we establish formulas for the cross sections of reactions $e^+e^- \to H^{++}H^{--}$ in collision energies from 1–3 TeV and calculate the number of events for DCH creation. These cross sections and the Higgs masses are represented as functions of very convenient parameters such as the masses of neutral CP-odd Higgses, the mass of the heavy singly charged gauge boson, and $\tan\gamma$ and $\tan\beta$ as ratios of Higgs vacuum expectation values (VEV), which will be defined in the work. This will help one more easily predict many properties relating to the DCHs as well as relations among the masses of particles in the model. With each collision energy level of 1.5, 2, and 3 TeV, we discuss the parameter space where the masses of three DCHs can satisfy the allowed kinetic condition; namely, the mass of each DCH must be smaller than half of the collision energy. Then we estimate the amplitudes of the cross sections in these regions of parameter space. Finally, the branching ratios of the DCH decay to pairs of same-sign leptons are briefly discussed.

2. Review of the SUSYRM331 model

This work is based on the models represented in Refs. [20,21]. For convenience, we summarize the important results that will be used in our calculation. Throughout this work, we will use the notation of the two-component spinor for fermions, where ψ denotes a particle and ψ^c denotes the corresponding antiparticle. Both ψ and ψ^c are left-handed spinors. In the case of Majorana fields, where $\psi = \psi^c$, we will use ψ notation.

2.1. Lepton and quark sectors

The lepton sector is arranged based on the original nonsupersymmetric version [13], namely,

$$\hat{L}_l = \left(\hat{\nu}, \quad \hat{l}, \quad \hat{l}^c\right)^T \sim (\mathbf{1}, \mathbf{3}, 0), \quad l = e, \mu, \tau. \tag{1}$$

The transformation properties under the respective factors $(\mathrm{SU}(3)_C,\ \mathrm{SU}(3)_L,\ \mathrm{U}(1)_X)$ appear in parentheses.

In the quark sector, the first quark family is put in a superfield that transforms as a triplet of the $\mathrm{SU}(3)_L$ group:

$$\hat{Q}_{1L} = \left(\hat{u}_1, \quad \hat{d}_1, \quad \hat{J}_1\right) \sim \left(\mathbf{3}, \mathbf{3}, \tfrac{2}{3}\right). \tag{2}$$

The three respective antiquark superfields are singlets of the $\mathrm{SU}(3)_L$ group:

$$\hat{u}^c_1 \sim \left(\mathbf{3}^*, \mathbf{1}, -\tfrac{2}{3}\right), \quad \hat{d}^c_1 \sim \left(\mathbf{3}^*, \mathbf{1}, \tfrac{1}{3}\right), \quad \hat{J}^c_1 \sim \left(\mathbf{3}^*, \mathbf{1}, -\tfrac{5}{3}\right). \tag{3}$$

The two remaining quark families are included in the two corresponding superfields, transforming as antitriplets:

$$\hat{Q}_{iL} = \left(\hat{d}_i, \quad -\hat{u}_i \quad \hat{j}_i\right)^T \sim \left(\mathbf{3}, \mathbf{3}^*, -\tfrac{1}{3}\right), \quad i = 2, 3. \tag{4}$$

and the respective antiquark superfields are singlets:

$$\hat{u}^c_i \sim \left(\mathbf{3}^*, \mathbf{1}, -\tfrac{2}{3}\right), \quad \hat{d}^c_i \sim \left(\mathbf{3}^*, \mathbf{1}, \tfrac{1}{3}\right), \quad \hat{j}^c_i \sim \left(\mathbf{3}^*, \mathbf{1}, \tfrac{4}{3}\right), \quad i = 2, 3. \tag{5}$$

The SUSYRM331 needs four Higgs superfields in order to generate all masses of leptons and quarks, but radiative corrections [20] or effective operators [21] must be added. For convenience in investigating the couplings between leptons and DCHs, in this work we will use the effective approach.

2.2. Gauge bosons and lepton–lepton–gauge boson vertices

The gauge boson sector of the SUSYRM331 model was thoroughly investigated in Refs. [20,21] and this sector is similar to that of the non-SUSY version [12]. According to these works, the gauge sector includes three neutral (A, Z, Z'), four singly charged $\left(W^{\pm}, V^{\pm}\right)$, and two doubly charged $U^{\pm\pm}$ gauge bosons. Of these, A, Z, and $W^{\pm}$ are SM particles, while the rest are $\mathrm{SU}(3)_L$ particles with masses being on the $\mathrm{SU}(3)_L$ scale. The new charged gauge bosons $V^{\pm}$ and $U^{\pm\pm}$ have a lepton number of two; hence, they are also called bileptons. According to the analysis in Ref. [73], the mass of the charged bilepton U is always less than $0.5 m_{Z'}$. Therefore, we expect the decays $Z' \to U^{++}U^{--}$ and $U^{\pm\pm} \to 2l^{\pm} (l = e, \mu, \tau)$ to be allowed, leading to spectacular signals in future colliders. The DCHs are also bileptons, leading to a very interesting consequence: the lightest DCH may be the lightest bilepton; it only decays to a charged lepton pair. This is exactly the case in the SUSYRM331, as we will prove through this work. All the masses of the gauge bosons can be written as functions of the W and V gauge boson masses. There is a simple relation between m_W, m_V, and m_U, namely, $m_U^2 = m_W^2 + m_V^2$, which will be summarized in the Higgs sector. Therefore, we can define m_V as a parameter characterized for the $SU(3)_L$ scale. Recently, the studies of flavor-neutral changing-current processes and the muon anomalous magnetic moment in the reduced minimal 3-3-1 model [74,75] have set the lower limits of m_V, namely, $m_V \geq 650$ and 910 GeV, respectively.

The vertex of ffV, which is very important in studying the creation of DCHs in e^+e^- colliders, is represented in the Lagrangian shown in Refs. [12,20,21,58], namely,

$$\mathcal{L}_{ffV} = g\bar{L}\bar{\sigma}^{\mu}\frac{\lambda^a}{2}LV_{\mu}^a. \tag{6}$$

The relations between the mass and the original states of neutral gauge bosons are given as follows:

$$\begin{pmatrix} W_{3\mu} \\ W_{8\mu} \\ B_{\mu} \end{pmatrix} = \mathcal{C}_{\rm B}\begin{pmatrix} A_{\mu} \\ Z_{\mu} \\ Z'_{\mu} \end{pmatrix}$$
$$= \begin{pmatrix} \frac{t}{\sqrt{2(2t^2+3)}}, & \frac{\sqrt{3}}{2}\left(c_{\zeta} + \frac{s_{\zeta}}{\sqrt{2t^2+3}}\right), & \frac{\sqrt{3}}{2}\left(-s_{\zeta} + \frac{c_{\zeta}}{\sqrt{2t^2+3}}\right) \\ -\frac{\sqrt{3}t}{\sqrt{2(2t^2+3)}} & \frac{1}{2}\left(c_{\zeta} - \frac{3s_{\zeta}}{\sqrt{2t^2+3}}\right), & -\frac{1}{2}\left(s_{\zeta} + \frac{3c_{\zeta}}{\sqrt{2t^2+3}}\right) \\ \frac{\sqrt{3}}{\sqrt{2t^2+3}} & -\frac{\sqrt{2}s_{\zeta}t}{\sqrt{2t^2+3}} & -\frac{\sqrt{2}c_{\zeta}t}{\sqrt{2t^2+3}} \end{pmatrix}\begin{pmatrix} A_{\mu} \\ Z_{\mu} \\ Z'_{\mu} \end{pmatrix}. \tag{7}$$

Here $c_{\zeta} \equiv \cos\zeta > 0$, $s_{\zeta} \equiv \sin\zeta > 0$ with ζ satisfying

$$\tan 2\zeta \equiv \frac{\sqrt{(3+2t^2)}(m_V^2 - m_W^2)}{(1+t^2)(m_V^2 + m_W^2)}. \tag{8}$$

The parameter t is the ratio between g' and g, namely,

$$t \equiv \frac{g'}{g} = \sqrt{\frac{6\sin^2\theta_W}{1-4\sin^2\theta_W}}. \tag{9}$$

The masses of gauge bosons are given by

$$\begin{aligned} m_{\gamma} &= 0, \\ m_Z^2 &= \frac{t^2+2}{3}\left(m_U^2 - \sqrt{m_U^4 - \frac{4(2t^2+3)}{(t^2+2)^2}m_V^2 m_W^2}\right), \\ m_{Z'}^2 &= \frac{t^2+2}{3}\left(m_U^2 + \sqrt{m_U^4 - \frac{4(2t^2+3)}{(t^2+2)^2}m_V^2 m_W^2}\right). \end{aligned} \tag{10}$$

The Z–Z' mixing angle in the framework of the RM331 model is quite small, $|\phi| < 10^{-3}$ [58]. It is interesting to note that, due to the generation discrimination in the 3-3-1 models, the new neutral gauge boson Z' has a flavor-changing neutral current [76–78].

Table 1. Vertex factors between leptons, quarks, and neutral gauge bosons. Note that $e = g\sin\theta_W$.

$\bar{f}fV_\mu$	A_μ	Z_μ	Z'_μ
ν_e	0	$\frac{igc_\zeta}{\sqrt{3}}\bar{\sigma}^\mu$	$\frac{-igs_\zeta}{\sqrt{3}}\bar{\sigma}^\mu$
e	$-ie$	$-\frac{ig}{2\sqrt{3}}\left(c_\zeta + \frac{3s_\zeta}{\sqrt{2t^2+3}}\right)\bar{\sigma}^\mu$	$\frac{ig}{2\sqrt{3}}\left(s_\zeta - \frac{3c_\zeta}{\sqrt{2t^2+3}}\right)\bar{\sigma}^\mu$
e^c	ie	$-\frac{ig}{2\sqrt{3}}\left(c_\zeta - \frac{3s_\zeta}{\sqrt{2t^2+3}}\right)\bar{\sigma}^\mu$	$\frac{ig}{2\sqrt{3}}\left(s_\zeta + \frac{3c_\zeta}{\sqrt{2t^2+3}}\right)\bar{\sigma}^\mu$
u	$\frac{i2e}{3}$	$\frac{ig}{\sqrt{3}}\left(c_\zeta - \frac{2t^2s_\zeta}{3\sqrt{2t^2+3}}\right)\bar{\sigma}^\mu$	$\frac{-ig}{\sqrt{3}}\left(s_\zeta + \frac{2t^2c_\zeta}{3\sqrt{2t^2+3}}\right)\bar{\sigma}^\mu$
u^c	$-\frac{i2e}{3}$	$\frac{2igt^2s_\zeta}{3\sqrt{3(2t^2+3)}}\bar{\sigma}^\mu$	$\frac{2igt^2c_\zeta}{3\sqrt{3(2t^2+3)}}\bar{\sigma}^\mu$
d	$-\frac{ie}{3}$	$-\frac{ig}{2\sqrt{3}}\left(c_\zeta + \frac{(4t^2+9)s_\zeta}{3\sqrt{2t^2+3}}\right)\bar{\sigma}^\mu$	$\frac{ig}{2\sqrt{3}}\left(s_\zeta - \frac{(4t^2+9)c_\zeta}{3\sqrt{2t^2+3}}\right)\bar{\sigma}^\mu$
d^c	$\frac{ie}{3}$	$-\frac{igt^2s_\zeta}{3\sqrt{3(2t^2+3)}}\bar{\sigma}^\mu$	$-\frac{igt^2c_\zeta}{3\sqrt{3(2t^2+3)}}\bar{\sigma}^\mu$
J_1	$\frac{5ie}{3}$	$-\frac{ig}{2\sqrt{3}}\left(c_\zeta + \frac{(4t^2-9)s_\zeta}{3\sqrt{2t^2+3}}\right)\bar{\sigma}^\mu$	$\frac{ig}{2\sqrt{3}}\left(s_\zeta + \frac{(4t^2-9)c_\zeta}{3\sqrt{2t^2+3}}\right)\bar{\sigma}^\mu$
J_1^c	$-\frac{5ie}{3}$	$\frac{5igt^2s_\zeta}{3\sqrt{3(2t^2+3)}}\bar{\sigma}^\mu$	$\frac{5igt^2c_\zeta}{3\sqrt{3(2t^2+3)}}\bar{\sigma}^\mu$
c, t	$\frac{i2e}{3}$	$\frac{ig}{2\sqrt{3}}\left(c_\zeta + \frac{(2t^2+9)s_\zeta}{3\sqrt{2t^2+3}}\right)\bar{\sigma}^\mu$	$\frac{-ig}{2\sqrt{3}}\left(s_\zeta - \frac{(2t^2+9)c_\zeta}{3\sqrt{2t^2+3}}\right)\bar{\sigma}^\mu$
c^c, t^c	$-\frac{i2e}{3}$	$\frac{2igt^2s_\zeta}{3\sqrt{3(2t^2+3)}}\bar{\sigma}^\mu$	$\frac{2igt^2c_\zeta}{3\sqrt{3(2t^2+3)}}\bar{\sigma}^\mu$
$s,\ b$	$-\frac{ie}{3}$	$-\frac{ig}{\sqrt{3}}\left(c_\zeta + \frac{t^2s_\zeta}{3\sqrt{2t^2+3}}\right)\bar{\sigma}^\mu$	$\frac{ig}{\sqrt{3}}\left(s_\zeta - \frac{4t^2c_\zeta}{3\sqrt{2t^2+3}}\right)\bar{\sigma}^\mu$
$s^c,\ b^c$	$\frac{ie}{3}$	$-\frac{igt^2s_\zeta}{3\sqrt{3(2t^2+3)}}\bar{\sigma}^\mu$	$-\frac{igt^2c_\zeta}{3\sqrt{3(2t^2+3)}}\bar{\sigma}^\mu$
$j_1,\ j_2$	$-\frac{4ie}{3}$	$-\frac{ig}{2\sqrt{3}}\left(c_\zeta + \frac{(2t^2-9)s_\zeta}{3\sqrt{2t^2+3}}\right)\bar{\sigma}^\mu$	$-\frac{ig}{2\sqrt{3}}\left(s_\zeta - \frac{(2t^2-9)c_\zeta}{3\sqrt{2t^2+3}}\right)\bar{\sigma}^\mu$
$j_1^c,\ j_2^c$	$\frac{4ie}{3}$	$-\frac{4igt^2s_\zeta}{3\sqrt{3(2t^2+3)}}\bar{\sigma}^\mu$	$-\frac{4igt^2c_\zeta}{3\sqrt{3(2t^2+3)}}\bar{\sigma}^\mu$

The above analysis is enough to calculate the vertex factors of charged leptons with neutral gauge bosons, as shown explicitly in Table 1. Here we only concentrate on the largest vertex couplings by assuming that the flavor basis of leptons and quarks is the mass basis.

2.3. *Constraint from the ρ parameter*

The above analysis shows that the structure of the neutral gauge bosons is the same as that of the RM331 model when all mixing and mass parameters of these bosons are written in terms of the charged gauge boson masses. So the contributions of new heavy gauge bosons to the ρ parameter from the $SU(3)_L$ charged gauge bosons are given in Refs. [79,80]. They also relate to the T parameter through the equality $\Delta\rho \equiv \rho - 1 \simeq \widehat{\alpha}(m_Z)T$, where $\widehat{\alpha}(m_Z)$ is the fine structure constant defined in the minimal scheme ($\overline{MS}$) at the m_Z scale [81]. The problem is that all of these contributions are always positive, so the total always makes the value of $\Delta\rho$ larger than the current experimental upper bound, unless the $SU(3)_L$ scale is larger than 9 TeV [62].

Because the new quarks are $SU(2)_L$ singlets, they do not contribute to the ρ parameters. The other contributions arise from Higgses and SUSY particles, including Higgsinos, gauginos, and superpartners of the fermions. Being functions of the SUSY parameters, they are completely independent of the $SU(3)_L$ scale. The contributions of the DCHs are only from the couplings [65]

$$ic\phi_1^*\partial_\mu\phi_2 V^\mu + h.c \quad (V = W, Z) \tag{11}$$

of two charged Higgses ϕ_1 and ϕ_2. According to Table C1, there are only nonzero vertices of $\chi^{++}W^-H_2^-$ and $\chi'^{++}W^-H_2^-$ related to DCHs. Because $\chi^{\pm\pm}$ and $\chi'^{\pm\pm}$ contribute mainly to $H_1^{\pm\pm}$ and the Goldstone $U^\pm$ boson, they mix with the other two DCHs with very small factors of orders smaller than $\mathcal{O}\left(\frac{m_W^3}{m_V^3}\right)$. In addition, the kind of interactions given in (11) with two identical DCHs gives zero contribution to the ρ parameter [65]. So the total contribution of the physical DCHs to the ρ parameter is strongly suppressed.

Because the Higgs triplets ρ and ρ' break $SU(2)_L$ symmetry, they will give the main contributions to the couplings of singly charged and neutral Higgses to normal gauge bosons and therefore may significantly affect the ρ parameter. This is very similar to the case of the MSSM. In fact, the SUSYRM331 contains two CP-even neutral Higgses and two singly charged Higgses $H_1^\pm$, which behave in the same way as those in the MSSM. More explicitly, they couple with the W and Z bosons in the same way as those in the MSSM, especially in the large limit of the $SU(3)_L$ and soft SUSY breaking scales, which is exactly the valid condition of the SUSYRM331. So the total contribution to the ρ parameter of these SUSYRM331 Higgses is nearly the same as what is found in the MSSM. In general, the contributions to the ρ parameter obtained from the investigation into the MSSM can also be used for the SUSY331 version [65]. The most important results are: i) all unexpected positive contributions decrease rapidly to zero when the overall sparticle mass scale is large enough, ii) the negative contribution from the Higgs scalars can reach absolute values of 10^{-4}, which is the order of the recent sensitive experimental value of the ρ parameter. In the SUSYRM331 framework, the total positive SUSY contribution can be set to the order of $\mathcal{O}(10^{-4})$, because the soft parameters are at least of the order of the $SU(3)_L$ scale, i.e., the TeV scale, while the total contribution from the Higgs scalar is completely different. It has a negative value when the masses of CP-odd neutral Higgses are very large and the lightest CP-even neutral Higgs reaches its largest value of $M_Z|\cos 2\beta|$ at the tree level [65,82][1]. Then, the contribution from the Higgs sector is

$$\Delta\rho_{\rm H}^{\rm susy} = \frac{3\alpha}{16\pi^2\sin^2\theta_W} f_H\left(\cos^2 2\beta, \theta_W\right), \tag{12}$$

where

$$f_H(x, \theta_W) \equiv x\left(\frac{\ln\left(\cos^2\theta_W/x\right)}{\cos^2\theta_W - x} + \frac{\ln x}{\cos^2\theta_W(1-x)}\right).$$

[1] Note that the well known β in the MSSM is different from our definition of β in (23). In fact, the γ parameter in (23) plays the same role as β in the MSSM.

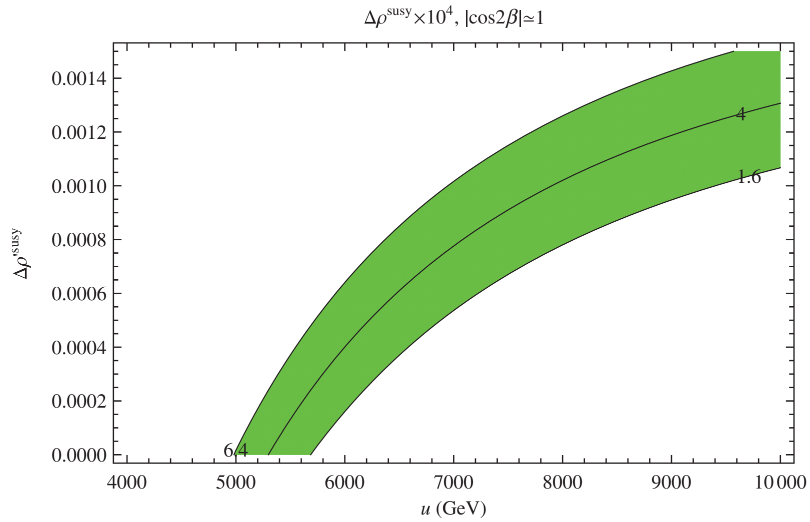

Fig. 1. Contour plot of $\Delta\rho^{\text{susy}}$ as a function of $\Delta\rho'^{\text{susy}}$ and the $SU(3)_L$ scale u. The green region satisfies $1.6 \times 10^{-4} \le \Delta\rho^{\text{susy}} \le 6.4 \times 10^{-4}$.

In the following, we will show that a negative $\Delta\rho_{\text{H}}^{\text{susy}}$ can cancel the new positive contributions arising from the SUSY and 3-3-1 properties. The total deviation of the ρ parameter can be divided into three parts,

$$\Delta\rho^{\text{susy}} = \widehat{\alpha}(m_Z)T_{\text{min}} + \Delta\rho_{\text{H}}^{\text{susy}} + \Delta\rho'^{\text{susy}}, \tag{13}$$

where $\Delta\rho'^{\text{susy}}$ is the total positive contribution of the Higgsino, gaugino, and sfermion particles, and T_{min} is the contribution from the minimal 3-3-1 framework to the oblique T parameter [79,80],

$$T_{\text{min}} = \frac{3\sqrt{2}G_F}{16\pi^2\widehat{\alpha}(m_Z)}\left[m_U^2 + m_V^2 - \frac{2m_U^2 m_V^2}{m_U^2 - m_V^2}\ln\frac{m_U^2}{m_V^2}\right] + \frac{1}{4\pi\sin^2\theta_W}\left[2 - \frac{m_U^2 m_V^2}{m_U^2 - m_V^2}\ln\frac{m_U^2}{m_V^2} + 3\tan^2\theta_W \ln\frac{m_U^2}{m_V^2}\right] + \frac{m_Z^2 - m_{Z_0}^2}{\widehat{\alpha}(m_Z)m_Z^2}, \tag{14}$$

where m_Z, $m_{Z'}$, m_U, and m_V are the masses of gauge bosons predicted by the SUSYRM331. All of the experimental values are given in Ref. [81], namely, $m_{Z_0} = 91.1876 \pm 0.0021$ GeV, $m_W = 80.385 \pm 0.015$ GeV, $\sin^2\theta_W = 0.231\,26$, $G_F = 1.166\,3878(6) \times 10^{-5}$ GeV^{-2}, and $\widehat{\alpha}^{-1}(m_Z) = 127.940 \pm 0.014$. Also, the experimental constraint of new physics to $\Delta\rho$ is $1.6 \times 10^{-4} \le \Delta\rho \le 6.4 \times 10^{-4}$ [81]. $\Delta\rho^{\text{susy}}$ is now a function of $|\cos 2\beta|$, $\Delta\rho'^{\text{susy}}$, and the $SU(3)_L$ scale $u = \sqrt{w^2 + w'^2}$. With the discovery of the neutral CP-even Higgs with a mass of 125 GeV, β should satisfy $|\cos 2\beta| \to 1$. The numerical result of $\Delta\rho^{\text{susy}}$ is shown in Fig. 1, where a lower bound of $u \ge 5$ TeV is allowed.

Finally, what we stress here is that the sum of the respective negative and positive contributions from $\Delta\rho_H^{\text{susy}}$ and $\Delta\rho'^{\text{susy}}$ is enough to keep the value of the ρ parameter within the allowed constraint. Therefore, unlike the non-SUSY version, in the SUSY view, the $SU(3)_L$ scale is free from the constraint of the ρ parameter.

On the other hand, the $\mathrm{SU}(3)_L$ scale is constrained by investigating the Z' boson. According to (10), we get

$$m_{Z'} \simeq \frac{2m_V c_W}{\sqrt{3\left(1-4\sin^2\theta_W\right)}}$$

in the limit of $u \gg v, v'$.

In the framework of the minimal 3-3-1 models, the investigation of the LEP-II constraints on $m_{Z'}$ [61] as well as the $B_d \to K^*\mu\mu$ data at LHC indicates that the lower bounds of $m_{Z'}$ must be above 7 TeV [83–85]. In addition, the above discussion suggests that the Z' boson in the SUSYRM331 model behaves similarly to the one in the non-SUSY version at the tree level. Combining this with the constraint of $m_{Z'}$ in order to avoid the Landau pole, the SUSYRM331 model predicts that the most interesting range of $m_{Z'}$ is $7\,\mathrm{TeV} \le m_{Z'} \le 9\,\mathrm{TeV}$, leading to $2\,\mathrm{TeV} \le m_V \le 3\,\mathrm{TeV}$.

2.4. Higgs sector

The scalar superfields, which are necessary to generate the fermion masses, are

$$\hat{\rho} = \begin{pmatrix} \hat{\rho}^+ \\ \hat{\rho}^0 \\ \hat{\rho}^{++} \end{pmatrix} \sim (\mathbf{1}, \mathbf{3}, +1), \quad \hat{\chi} = \begin{pmatrix} \hat{\chi}^- \\ \hat{\chi}^{--} \\ \hat{\chi}^0 \end{pmatrix} \sim (\mathbf{1}, \mathbf{3}, -1). \tag{15}$$

To remove the chiral anomalies generated by the superpartners of the scalars, two new scalar superfields are introduced to transform as antitriplets under the $\mathrm{SU}(3)_L$, namely,

$$\hat{\rho}' = \begin{pmatrix} \hat{\rho}'^- \\ \hat{\rho}'^0 \\ \hat{\rho}'^{--} \end{pmatrix} \sim (\mathbf{1}, \mathbf{3}^*, -1), \quad \hat{\chi}' = \begin{pmatrix} \hat{\chi}'^+ \\ \hat{\chi}'^{++} \\ \hat{\chi}'^0 \end{pmatrix} \sim (\mathbf{1}, \mathbf{3}^*, +1). \tag{16}$$

The pattern of the symmetry breaking of the model is given by the following scheme (using the notation given in Ref. [86]):

$$\begin{aligned} \text{SUSYRM331} &\overset{\mathcal{L}_{\text{soft}}}{\longmapsto} \mathrm{SU}(3)_C \otimes \mathrm{SU}(3)_L \otimes \mathrm{U}(1)_X \\ &\overset{\langle\chi\rangle\langle\chi'\rangle}{\longmapsto} \mathrm{SU}(3)_C \otimes \mathrm{SU}(2)_L \otimes \mathrm{U}(1)_Y \\ &\overset{\langle\rho\rangle\langle\rho'\rangle}{\longmapsto} \mathrm{SU}(3)_C \otimes \mathrm{U}(1)_Q. \end{aligned} \tag{17}$$

For the sake of simplicity, all vacuum expectation values (VEVs) are supposed to be real. When the 3-3-1 symmetry is broken, i.e., $\mathrm{SU}(3)_C \otimes \mathrm{U}(1)_Q$, the VEVs of the scalar fields are defined as follows:

$$\begin{aligned} \langle\rho\rangle &= \left(0, \quad \frac{v}{\sqrt{2}}, \quad 0\right)^T, \quad \langle\chi\rangle = \left(0, \quad 0, \quad \frac{w}{\sqrt{2}}\right)^T, \\ \langle\rho'\rangle &= \left(0, \quad \frac{v'}{\sqrt{2}}, \quad 0\right)^T, \quad \langle\chi'\rangle = \left(0, \quad 0, \quad \frac{w'}{\sqrt{2}}\right)^T. \end{aligned} \tag{18}$$

Because the symmetry breaking happens through the steps given in (17), the VEVs have to satisfy the condition $w, w' \gg v, v'$. The constraint on the W boson mass leads to the consequence that

$$V^2 \equiv v^2 + v'^2 = (246\,\mathrm{GeV})^2. \tag{19}$$

2.5. Higgs spectra

As usual, the scalar Higgs potential is written as in Ref. [20], except for V_{soft}, which is added to the b-type terms [21] to guarantee the vacuum stability of the model and to avoid the appearance of many tachyon scalars [87,88]. Therefore, we have

$$V_{\text{SUSYRM331}} = V_{\text{D}} + V_{\text{F}} + V_{\text{soft}} \tag{20}$$

with

$$\begin{aligned}
V_{\text{D}} &= -\mathcal{L}_D = \frac{1}{2}\left(D^a D^a + DD\right)\\
&= \frac{g'^2}{12}(\bar{\rho}\rho - \bar{\rho'}\rho' - \bar{\chi}\chi + \bar{\chi'}\chi')^2 + \frac{g^2}{8}\sum_{i,j}\left(\bar{\rho}_i\lambda^a_{ij}\rho_j + \bar{\chi}_i\lambda^a_{ij}\chi_j - \bar{\rho'}_i\lambda^{*a}_{ij}\rho'_j - \bar{\chi'}_i\lambda^{*a}_{ij}\chi'_j\right)^2,\\
V_{\text{F}} &= -\mathcal{L}_F = \sum_F \bar{F}_\mu F_\mu = \sum_i\left[\left|\frac{\mu_\rho}{2}\rho'_i\right|^2 + \left|\frac{\mu_\chi}{2}\chi'_i\right|^2 + \left|\frac{\mu_\rho}{2}\rho_i\right|^2 + \left|\frac{\mu_\chi}{2}\chi_i\right|^2\right],\\
V_{\text{soft}} &= -\mathcal{L}_{\text{SMT}} = m^2_\rho\bar{\rho}\rho + m^2_\chi\bar{\chi}\chi + m^2_{\rho'}\bar{\rho'}\rho' + m^2_{\chi'}\bar{\chi'}\chi' - \left(b_\rho\rho\rho' + b_\chi\chi\chi' + \text{h.c.}\right),
\end{aligned} \tag{21}$$

where m_ρ, m_χ, $m_{\rho'}$, and $m_{\chi'}$ have the mass dimension. Both b_ρ and b_χ have a squared mass dimension and are assumed to be real and positive to ensure nonzero and real values for the VEVs. The expansions of the neutral scalars around their VEVs are

$$\begin{aligned}
\langle\rho\rangle &= \frac{1}{\sqrt{2}}\begin{pmatrix}0\\ v + H_\rho + iF_\rho\\ 0\end{pmatrix}, \quad \langle\rho'\rangle = \frac{1}{\sqrt{2}}\begin{pmatrix}0\\ v' + H_{\rho'} + iF_{\rho'}\\ 0\end{pmatrix},\\
\langle\chi\rangle &= \frac{1}{\sqrt{2}}\begin{pmatrix}0\\ 0\\ w + H_\chi + iF_\chi\end{pmatrix}, \quad \langle\chi'\rangle = \frac{1}{\sqrt{2}}\begin{pmatrix}0\\ 0\\ w' + H_{\chi'} + iF_{\chi'}\end{pmatrix}.
\end{aligned} \tag{22}$$

The minimum of the Higgs potential corresponds to the vanishing of all linear Higgs terms in the above potential. As a result, it leads to four independent equations, shown in Ref. [21], which reduce to four independent parameters in the original Higgs potential. We will use the notations chosen in Ref. [20] for this work. In particular, two independent parameters are chosen as

$$t_\gamma = \tan\gamma = \frac{v}{v'}, \quad t_\beta = \tan\beta = \frac{w}{w'}. \tag{23}$$

These are two ratios of the VEVs of neutral Higgs scalars, and similar to the β parameter defined in the MSSM. The two electroweak and $SU(3)_L$ scales relate to the masses of the W and V bosons [20,21] by two equations:

$$m^2_W = \frac{g^2}{4}\left(v^2 + v'^2\right); \quad m^2_V = \frac{g^2}{4}\left(w^2 + w'^2\right).$$

We can choose m_V as an independent parameter. On the other hand, there are two heavy doubly charged bosons, denoted as $U^{\pm\pm}$, with mass m_U satisfying $m^2_U = m^2_V + m^2_W$. If $m_V \gg m_W$, there will appear a degeneration of two heavy boson masses, $m_U = m_V + \frac{1}{2}m_W \times \mathcal{O}(m_W/m_V) + m_W \times \mathcal{O}(m_W/m_V)^3 \simeq m_V$. As mentioned above, the constraint of m_V gives a very small ratio between the two scales $SU(2)_L$ and $SU(2)_L$: $m_W^2/m_V^2 \leq \mathcal{O}(10^{-3})$. This is a rather good limit for the approximation used in this work. The minimum conditions of the superpotential result in a series of four equations:

$$m_\rho^2 + \frac{1}{4}\mu_\rho^2 = \frac{b_\rho}{t_\gamma} - \frac{1+t^2}{3} \times m_V^2 \cos 2\beta + \frac{t^2+2}{3} \times m_W^2 \cos 2\gamma, \tag{24}$$

$$m_\chi^2 + \frac{\mu_\chi^2}{4} = \frac{b_\chi}{t_\beta} - \frac{2+t^2}{3} \times m_V^2 \cos 2\beta + \frac{1+t^2}{3} \times m_W^2 \cos 2\gamma, \tag{25}$$

$$s_{2\gamma} \equiv \sin 2\gamma = \frac{2b_\rho}{m_\rho^2 + m_{\rho'}^2 + \frac{1}{2}\mu_\rho^2}, \quad s_{2\beta} \equiv \sin 2\beta = \frac{2b_\chi}{m_\chi^2 + m_{\chi'}^2 + \frac{1}{2}\mu_\chi^2}. \tag{26}$$

The two equations in (26) show the relations between the soft parameters and the ratios of the VEVs, and they are much the same as those shown in the MSSM. To estimate the scale of these soft parameters, based on the calculation in Ref. [38] it is useful to write Eqs. (24) and (25) in new forms, as follows:

$$c_{2\gamma} \equiv \cos 2\gamma = \frac{-\left(m_\chi^2 + \frac{\mu_\chi^2}{4} - \frac{b_\chi}{t_\beta}\right)\left(1+2s_W^2\right) + 2\left(m_\rho^2 + \frac{\mu_\rho^2}{4} - \frac{b_\rho}{t_\gamma}\right)c_W^2}{m_W^2}, \tag{27}$$

$$\begin{aligned} c_{2\beta} \equiv \cos 2\beta &= \frac{\left(m_\rho^2 + \frac{\mu_\rho^2}{4} - \frac{b_\rho}{t_\gamma}\right)\left(1+2s_W^2\right) - 2\left(m_\chi^2 + \frac{\mu_\chi^2}{4} - \frac{b_\chi}{t_\beta}\right)c_W^2}{m_V^2} \\ &= \frac{m_W^2}{m_V^2} \times \frac{(1+3t_W^2)c_{2\gamma}}{2} - \frac{3\left(1-4s_W^2\right)}{2c_W^2} \times \frac{\left(m_\chi^2 + \frac{\mu_\chi^2}{4} - \frac{b_\chi}{t_\beta}\right)}{m_V^2}. \end{aligned} \tag{28}$$

Because $|c_{2\gamma}| \leq 1$, Eq. (27) results in a consequence: $\left| -\left(m_\chi^2 + \frac{\mu_\chi^2}{4} - \frac{b_\chi}{t_\beta}\right)\left(1+2s_W^2\right) + 2\left(m_\rho^2 + \frac{\mu_\rho^2}{4} - \frac{b_\rho}{t_\gamma}\right)c_W^2 \right| \leq m_W^2$. However, the soft-breaking parameters, such as m_χ^2, m_ρ^2, b_χ, b_ρ, should be much larger than m_W^2, so these parameters must be degenerate. In addition, the left-hand side of (28) also has an upper bound, $|c_{2\beta}| \leq 1$, as does the right-hand side. Because of the hierarchy between the two breaking scales $SU(3)_L$ and $SU(2)_L$, $m_W \ll m_V$, the first term on the right-hand side is suppressed, and then we have $\left|\left(m_\chi^2 + \frac{\mu_\chi^2}{4} - \frac{b_\chi}{t_\beta}\right)\right| \leq \frac{2c_W^2}{3\left(1-4s_W^2\right)} m_V^2$. Hence, the two quantities $\left(m_\chi^2 + \frac{\mu_\chi^2}{4} - \frac{b_\chi}{t_\beta}\right)$ and $\left(m_\rho^2 + \frac{\mu_\rho^2}{4} - \frac{b_\rho}{t_\gamma}\right)$ are all in the $SU(3)_L$ scale. This leads to an interesting constraint on the soft-breaking parameters of the SUSYRM331: Although the supersymmetry is spontaneously broken before the breaking of the $SU(3)_L$ symmetry, both the soft parameters and the $SU(3)_L$ breaking scale should be of the same order. This is a very interesting point that is not mentioned in Ref. [21]. This conclusion also explains why the values of parameters b_ρ and b_χ in Ref. [21] are chosen in order to get consistent values of the lightest CP-even neutral Higgs mass.

Although the Higgs sector of the SUSYRM331 was investigated in Ref. [21], the two squared mass matrices of neutral Higgses and DCHs are only numerically estimated with some specific values of parameter space. However, we think that, before starting a numerical calculation, it is better to find approximate expressions of these masses in order to predict reasonable ranges of the parameters in the model, as we will show in this work. More importantly, we will show that approximate expressions are very useful in determining many interesting properties of the Higgs spectra.

The Higgs spectra are listed as follows:

(1) **CP-odd neutral Higgses**. Two massless Higgses eaten by two neutral gauge bosons are

$$H_{A_3} = F_{\chi'} \cos\beta - F_{\chi} \sin\beta, \quad H_{A_4} = F_{\rho'} \cos\gamma - F_{\rho} \sin\gamma. \tag{29}$$

Two massive Higgses are expressed in terms of the original Higgses, as follows:

$$H_{A_1} = F_{\rho} \cos\gamma + F_{\rho'} \sin\gamma, \quad H_{A_2} = F_{\chi} \cos\beta + F_{\chi'} \sin\beta$$

and their masses are

$$m^2_{A_1} = \frac{2b_\rho}{s_{2\gamma}} = m^2_\rho + m^2_{\rho'} + \frac{1}{2}\mu^2_\rho, \quad m^2_{A_2} = \frac{2b_\chi}{s_{2\beta}} = m^2_\chi + m^2_{\chi'} + \frac{1}{2}\mu^2_\chi. \tag{30}$$

(2) **Singly charged Higgses**. Two massless eigenstates of these Higgses are

$$H^\pm_3 = \chi^\pm \sin\beta + \chi'^\pm \cos\beta, \quad H^\pm_4 = \rho^\pm \sin\gamma + \rho'^\pm \cos\gamma,$$

which are eaten by the singly charged gauge bosons. Two other massive states are

$$\begin{aligned} H^\pm_1 &= -\rho^\pm \cos\gamma + \rho'^\pm \sin\gamma, \quad m^2_{H^\pm_1} = m^2_{A_1} + m^2_W, \\ H^\pm_2 &= -\chi^\pm \cos\beta + \chi'^\pm \sin\beta, \quad m^2_{H^\pm_2} = m^2_{A_2} + m^2_V. \end{aligned} \tag{31}$$

(3) **CP-even neutral Higgses**. In the basis of $(H_\rho, H_{\rho'}, H_\chi, H_{\chi'})$, the mass term of the neutral scalar Higgses has the form of

$$\mathcal{L}_{H^0} = \tfrac{1}{2}(H_\rho, H_{\rho'}, H_\chi, H_{\chi'}) \times \mathcal{M}^2_{4H} \times (H_\rho, H_{\rho'}, H_\chi, H_{\chi'})^T, \tag{32}$$

where

$$M^2_{4H} = \begin{pmatrix} m^2_{S11} & m^2_{S12} & m^2_{S13} & m^2_{S14} \\ & m^2_{S22} & m^2_{S23} & m^2_{S24} \\ & & m^2_{S33} & m^2_{S34} \\ & & & m^2_{S44} \end{pmatrix}.$$

Analytic formulas for the entries in the matrix were listed in Refs. [20,21]. There is a problem with finding exact analytic expressions for the eigenvalues with this matrix, which is why Ref. [21] had to choose the approach of numerical investigation.

We remind ourselves that the eigenvalues of this matrix, $\lambda = m^2_{H^0}$, must satisfy the equation

$$f(\lambda) \equiv \det\left(M^2_{4H} - \lambda I_4\right) = 0. \tag{33}$$

As a function of λ, the left-hand side of (33) is a polynomial of degree 4. Based on the very detailed discussion on Higgs spectra of the SUSYE331 in Ref. [38], which we will not repeat, this function can be expressed in terms of the independent parameters m_{A_1}, m_{A_2}, $c_{2\gamma}$, $c_{2\beta}$, m_W, and m_V, where m_{A_1} and m_{A_2} are soft-breaking parameters. As noted above, these soft parameters are of the same orders of the m_V–SU(3)$_L$ scale, i.e., m_{A_1}/m_V, $m_{A_2}/m_V \sim \mathcal{O}(1)$. To find approximate expressions for the Higgs masses, it is necessary to define a very small parameter: $\epsilon = \left(m_W^2/m_V^2\right) \leq (80.4/2000)^2 = 0.0016$. Then the masses of these neutral Higgses can be written as expansions of powers of ϵ:

$$m^2_{H^0_1} = M_Z^2 c^2_{2\gamma} + \mathcal{O}\left(m_W^2\right) \times \epsilon,$$
$$m^2_{H^0_2} = M^2_{A_1} + \mathcal{O}\left(m_W^2\right),$$
$$m^2_{H^0_{3,4}} = \frac{1}{6}\left[\frac{4c_W^2 m_V^2}{1-4s_W^2} + 3m^2_{A_2} \pm \sqrt{-\frac{48c^2_{2\beta}m^2_{A_2}m_V^2}{1-4s_W^2} + \left(3m^2_{A_2} + \frac{4c_W^2 m_V^2}{1-4s_W^2}\right)^2}\,\right] + \mathcal{O}\left(m_W^2\right). \tag{34}$$

It is necessary to note that the lightest mass has a tree-level value of $m_Z|\cos 2\gamma| \leq m_Z = 92$ GeV, consistent with the numerical result shown in Ref. [21]. Thus, the mass including loop corrections will increase to the current value of 125–126 GeV.

Although the Higgs sector was investigated in Ref. [21], we should emphasize a new feature in our work. To estimate the tree-level mass of the lightest CP-even Higgs, by using a reasonable approximation, we have obtained an analytic formula that is very consistent with that given in the MSSM. The interesting point is that our result depends only on the condition that all soft parameters must be in the SU(3)$_L$ scale. The result also suggests that the γ parameter in the SUSYRM331 model plays a very similar role to the β parameter in the MSSM, defined as the ratio of two VEVs. This approximation is very useful for estimating masses as well as predicting many interesting properties of the DCHs, as we will do in this work. The authors of Ref. [21] also considered only the top quark and its superpartner for investigating one-loop corrections to the mass of the lightest neutral Higgs, then used this allowed value to constrain the masses of the DCHs. However, unlike the MSSM, the SUSYRM331 contains new heavy exotic quarks and their superpartners, leading to the fact that their loop corrections to the mass of the lightest neutral Higgs have to be considered. Because the masses of these new quarks are arbitrary, one cannot tell much about the constraints of charged Higgs masses from considering these loop corrections.

The approximate formula (34) of neutral Higgs masses is useful for finding mass eigenstates of the neutral Higgses. We will consider the two following rotations for the squared mass matrix of neutral Higgses appearing in (32):

$$C_1^{\mathrm{n}} = \begin{pmatrix} -c_\gamma & s_\gamma & 0 & 0 \\ s_\gamma & c_\gamma & 0 & 0 \\ 0 & 0 & 1 & 0 \\ 0 & 0 & 0 & 1 \end{pmatrix}, \quad C_2^{\mathrm{n}} = \begin{pmatrix} 1 & 0 & 0 & 0 \\ 0 & c_\alpha & -s_\alpha & 0 \\ 0 & s_\alpha & c_\alpha & 0 \\ 0 & 0 & 0 & 1 \end{pmatrix}, \tag{35}$$

where $s_\alpha \equiv \sin\alpha$ and $c_\alpha \equiv \cos\alpha$ will be defined later. Taking the first rotation, we obtain

$$C_1^n M_{4H}^2 C_1^{nT} = \begin{pmatrix} m_{A_1}^2 + \frac{2c_{2\gamma}^2(t^2+2)}{3} m_W^2 & \frac{s_{4\gamma}(t^2+2)}{3} m_W^2 & \frac{2s_{2\gamma}s_\beta(t^2+1)}{3} m_W m_V & -\frac{2s_{2\gamma}c_\beta(t^2+1)}{3} m_W m_V \\ & \frac{2c_{2\gamma}^2(t^2+2)}{3} m_W^2 & \frac{2c_{2\gamma}s_\beta(t^2+1)}{3} m_W m_V & -\frac{2c_{2\gamma}c_\beta(t^2+1)}{3} m_W m_V \\ & & c_\beta^2 m_{A_2}^2 + \frac{2s_\beta^2(t^2+2)}{3} m_V^2 & s_{2\beta}\left[\frac{m_{A_2}^2}{2} + (t^2+2) m_V^2\right] \\ & & & s_\beta^2 m_{A_2}^2 + \frac{2c_\beta^2(t^2+2)}{3} m_V^2 \end{pmatrix}. \tag{36}$$

The first diagonal entry of (36) is equal to the largest contribution to $m^2_{H_2^0}$, and the submatrix, including entries $\left(C_1^n M_{4H}^2 C_1^{nT}\right)_{(i,j=4,5)}$, gives two other values of heavy masses $m^2_{H_3^0}$ and $m^2_{H_4^0}$, while the entry $\left(C_1^n M_{4H}^2 C_1^{nT}\right)_{33} = \frac{2c_{2\gamma}^2(t^2+2)}{3} m_W^2 = \mathcal{O}(m_W^2)$ relates to the lightest Higgs mass, but is different from that shown in (34). To get the right value, it must take more contributions from nondiagonal attempts containing factors $m_W m_V$ after taking other rotations. As mentioned above, the most interesting values of α and β satisfy $c_{2\gamma}, c_{2\beta} \to -1$, i.e., $s_{\gamma,\beta} \to 1$ and $c_{\gamma,\beta} \to 0$. This suggests that the largest correction to the lightest mass is from the entries $\left(C_1^n M_{4H}^2 C_1^{nT}\right)_{23}$ and $\left(C_1^n M_{4H}^2 C_1^{nT}\right)_{32}$. So, taking the second rotation with C_2^n given in (35) and using the limits $m_W^2 \ll m_V^2$ and $c_\beta \to 0$, it is easy to confirm that $\left(C_2^n C_1^n M_{4H}^2 (C_2^n C_1^n)^T\right)_{(22)} \simeq m_Z^2 |c_{2\gamma}|$ with α determined by

$$\tan 2\alpha \equiv \frac{4c_{2\gamma}s_\beta(t^2+1)m_W m_V}{3c_\beta^3 m_{A_2}^2 + 2s_\beta^2(t^2+2)m_V^2 - 2c_{2\gamma}^2(t^2+2)m_W^2} \sim \mathcal{O}(m_W/mV). \tag{37}$$

Then we can estimate that the contributions of the original Higgs states to the mass eigenstates of the CP-even neutral Higgses H_1^0 and H_2^0 are

$$H_\rho \to c_\alpha s_\gamma H_1^0 - c_\gamma H_2^0, \quad H_{\rho'} \to c_\alpha c_\gamma H_1^0 + s_\gamma H_2^0, \quad H_\chi, H_{\chi'} \to \mathcal{O}(s_\alpha) H_1^0. \tag{38}$$

It is interesting that, in the decoupling regime where the SUSY and $SU(3)_L$ scales are much larger than the $SU(2)_L$ scale, we have $H_\rho \simeq s_\gamma H_1^0 - c_\gamma H_2^0$ and $H_{\rho'} \simeq c_\gamma H_1^0 + s_\gamma H_2^0$, the same as those given in the MSSM [82]. Therefore, all couplings of these two Higgses with $W^\pm$ and Z bosons are the same as those in the MSSM. More interestingly, the SUSYRM331 contains a set of Higgses including $m_{H^0_{1,2}}$, m_{A_1}, and $m_{H_1^\pm}$ that has similar properties to the Higgs spectra of the MSSM. This property of the SUSY versions of the 3-3-1 models has also been indicated previously [38]. As a result, the SUSY Higgs contributions to the ρ parameter are the same in both MSSM and SUSYRM331 in the decoupling regime.

At the tree level, the above analysis indicates that the Higgs spectra can be determined by unknown independent parameters: γ, β, m_V, m_{A_1}, and m_{A_2}. Furthermore, the squared mass matrices of both CP-even neutral Higgses and DCHs depend explicitly on $c_{2\beta}, s_{2\beta}, c_{2\gamma}$, and $s_{2\gamma}$ but not $t_{2\gamma}, t_{2\beta}$. Hence, it can be guessed that the Higgs masses will not increase to infinity when t_γ and t_β are very large. In addition, in some cases, we can take the limits $c_{2\beta,2\gamma} \to -1$ and $s_{2\beta,2\gamma} \to 0$ without any inconsistent calculations. We will use the limit 2 TeV $\le m_V \le$ 3 TeV based on the latest update discussed above. m_{A_1} and m_{A_2} are of the same order of m_V so we set $m_{A_1}, m_{A_2} \ge 1$ TeV in our calculation. Other well known values that will be used are the mass of the W boson $m_W = 80.4$ GeV, the sine of the Weinberg angle $s_W = 0.231$, and the mass and total decay width of the Z boson $m_Z = 91.2$ GeV, $\Gamma_Z = 2.46$ GeV. The discovery of the lightest CP-even Higgs mass of 125 GeV implies that $|c_{2\gamma}| \simeq 1$, i.e., t_γ should be large enough, similar to the case of the MSSM. As a consequence, relation (27) shows the fine tuning among soft parameters and relation (28) predicts that $|c_{2\beta}|$ should also be large. Therefore, we will fix $t_\beta = 5$ and $t_\gamma = 10$ in the numerical investigation that can be applied for the general case of large t_β and t_γ. This can be understood from the reason that all quantities that we consider below depend on γ, 2γ, β, and 2β only by sine or cosine factors, not tan functions.

3. Doubly charged Higgs bosons and couplings

3.1. *Mass spectra and properties of the lightest DCH*

Consider the DCHs; the SUSYE331 model contains 8 degrees of freedom after final symmetry breaking. Therefore, the squared mass matrix is 4×4 and we cannot find the exact expressions for the physical masses. We will treat them the same as the neutral CP-even Higgses, in much more detail to discover all possible interesting properties of the DCHs, especially the lightest.

The mass term of the doubly charged boson is:

$$\mathcal{L}_{H^{\pm\pm}} = \left(\rho^{++}, \quad \rho'^{++}, \quad \chi^{++}, \quad \chi'^{++}\right) \mathcal{M}^2_{H^{\pm\pm}} \left(\rho^{--} \quad \rho'^{--} \quad \chi^{--} \quad \chi'^{--}\right)^T,$$

where the elements of the squared mass matrix were shown precisely in Ref. [21]. Taking a rotation characterized by a matrix

$$C_1 = \begin{pmatrix} \frac{-m_W s_\gamma}{m_U} & 0 & c_\gamma & \frac{m_V s_\gamma}{m_U} \\ \frac{-m_W c_\gamma}{m_U} & 0 & -s_\gamma & \frac{m_V c_\gamma}{m_U} \\ \frac{m_V s_\beta}{m_U} & -c_\beta & 0 & \frac{m_W s_\beta}{m_U} \\ \frac{m_V c_\beta}{m_U} & s_\beta & 0 & \frac{m_W c_\beta}{m_U} \end{pmatrix}, \tag{39}$$

we get new squared mass matrix:

$$\mathcal{M}^2_{H'^{\pm\pm}} \equiv C_1^T \mathcal{M}^2_{H^{\pm\pm}} C_1$$
$$= \begin{pmatrix} 0 & 0 & 0 & 0 \\ 0 & m^2_{A_2} + m^2_V - c_{2\beta}c_{2\gamma}m^2_W & -s_{2\beta}s_{2\gamma}m_V m_W & c_{2\gamma}s_{2\beta}m_U m_W \\ 0 & -s_{2\beta}s_{2\gamma}m_V m_W & m^2_{A_1} - c_{2\beta}c_{2\gamma}m^2_V + m^2_W & -s_{2\gamma}c_{2\beta}m_U m_V \\ 0 & c_{2\gamma}s_{2\beta}m_U m_W & -s_{2\gamma}c_{2\beta}m_U m_V & c_{2\gamma}c_{2\beta}m^2_U \end{pmatrix}. \tag{40}$$

Corresponding to the massless solution in (40), the Goldstone boson eaten by the doubly charged gauge boson is represented exactly in term of the original Higgses:

$$G^{\pm\pm} = -\frac{m_W s_\gamma}{m_U}\rho^{\pm\pm} - \frac{m_W c_\gamma}{m_U}\rho'^{\pm\pm} + \frac{m_V s_\beta}{m_U}\chi^{\pm\pm} + \frac{m_V c_\beta}{m_U}\chi'^{\pm\pm}. \tag{41}$$

Because $m_W \ll m_U$, $m_V \simeq m_U$, and $s_\gamma \leq 1$, the doubly charged gauge boson couples weakly to light Higgses but strongly to heavy Higgses.

The squared mass matrix of the DCHs (40) also shows that, if there exists a light DCH $\left(\text{i.e.}, \sim \mathcal{O}(m^2_W)\right)$, then the contributions of the off-diagonal entries to the mass of this Higgs are large. Then it is difficult to find an analytic formula for both mass eigenstates and eigenvalues. Note that, apart from the Goldstone boson (41), there are three other states denoted by $H_i'^{\pm\pm},\ (i = 1, 2, 3)$. They relate to the original DCHs by a transformation:

$$\left(\rho^{\pm\pm},\quad \rho'^{\pm\pm},\quad \chi^{\pm\pm},\quad \chi'^{\pm\pm}\right)^T = C_1\left(G^{\pm\pm},\quad H_1'^{\pm\pm},\quad H_2'^{\pm\pm},\quad H_3'^{\pm\pm}\right)^T. \tag{42}$$

We assume that the three physical DCHs relate to $(H_1'^{\pm\pm},\ H_2'^{\pm\pm},\ H_3'^{\pm\pm})$ by a 3×3 matrix Λ as follows:

$$\left(H_1'^{\pm\pm},\ H_2'^{\pm\pm},\ H_3'^{\pm\pm}\right)^T = \Lambda\left(H_1^{\pm\pm},\ H_2^{\pm\pm},\ H_3^{\pm\pm}\right)^T. \tag{43}$$

To estimate the values of the entries in the matrix Λ, we firstly find out some properties of the mass eigenvalues of the DCHs. The remaining three eigenvalues of this matrix $\lambda = m^2_{H^{\pm\pm}}$ must satisfy the equation $\det\left(\mathcal{M}^2_{H^{\pm\pm}} - \lambda I_4\right) = 0$, or, equivalently, $\lambda f(\lambda) = 0$ with

$$f(\lambda) = a\lambda^3 + b\lambda^2 + c\lambda + d, \tag{44}$$

where

$$\begin{aligned}
a &= -\left(m_V^2 + m_{A_1}^2 + m_{A_2}^2 + m_W^2\right),\\
b &= -c_{2\beta}^2 m_V^4 + m_{A_1}^2\left(m_V^2 + c_{2\beta}c_{2\gamma} + m_{A_2}^2\right) + \left[m_{A_2}^2 + c_{2\beta}c_{2\gamma}\left(2m_V^2 + m_{A_2}^2\right)\right] m_W^2 - c_{2\gamma}^2 m_W^4,\\
c &= \left(m_V^2 + m_W^2\right)\left[c_{2\beta}m_V^2 - c_{2\gamma}\left(m_W^2 + m_{A_1}^2\right)\right]\left[c_{2\beta}\left(m_V^2 + m_{A_2}^2\right) - c_{2\gamma}m_W^2\right].
\end{aligned} \tag{45}$$

This equation gives three solutions corresponding to three masses of the physical DCHs at the tree level. We denote them as $m^2_{H_i^{\pm\pm}}$ with $i = 1, 2, 3$ and $m^2_{H_1^{\pm\pm}}, m^2_{H_2^{\pm\pm}} > m^2_{H_3^{\pm\pm}}$. Combining the last equation of (45) with Vieta's formula, in order to avoid the appearance of tachyons, we deduce that

$$m^2_{H_1^{\pm\pm}} m^2_{H_2^{\pm\pm}} m^2_{H_3^{\pm\pm}} = -c > 0 \Longleftrightarrow \frac{\left(m_{A_1}^2 + m_W^2\right)c_{2\gamma}}{m_V^2} < c_{2\beta} < \frac{m_W^2 c_{2\gamma}}{m_V^2 + m_{A_2}^2} < 0. \tag{46}$$

Furthermore, the entry $()_{22}$ of (40) suggests that, if $m^2_{A_1}$ is enough close to m_V^2, there may appear one light DCH, while the other two values are always in the $SU(3)_L$ scale. So, in order to find the best approximate formulas of the vertex factors $V^0 H^{++} H^{--}$, it is better to investigate the mass values of the DCHs using the techniques shown in Ref. [38], and partly mentioned when discussing the neutral CP-even Higgs sector. The masses can be expanded as

$$m^2_{H^{\pm\pm}} = X' m_V^2 + X'' \times m_W^2 + \mathcal{O}(\epsilon) \times m_W^2. \tag{47}$$

The heavy Higgses satisfy the condition $X' \sim \mathcal{O}(1)$, i.e., in the soft-breaking or $SU(3)_L$ scale. Keeping only the leading term in (47) as the largest contribution, the masses of the three DCHs are

$$\begin{aligned}
m^2_{H_1^{\pm\pm}} &\simeq m_V^2 + m_{A_2}^2,\\
m^2_{H_{2,3}^{\pm\pm}} &\simeq \frac{1}{2}\left(m_{A_1}^2 \pm \sqrt{4c_{2\beta}^2 m_V^4 - 4c_{2\beta}c_{2\gamma}m_V^2 m_{A_1}^2 + m_{A_1}^4}\right).
\end{aligned} \tag{48}$$

Comparing the $\left(\mathcal{M}^2_{H'^{\pm\pm}}\right)_{33}$ entry of (40) with $m^2_{H_1^{\pm\pm}}$ in the first line of (48), it can be realized that $\left(\mathcal{M}^2_{H'^{\pm\pm}}\right)_{33} - m^2_{H_1^{\pm\pm}} = \mathcal{O}\left(m_W^2\right) \ll m^2_{H_1^{\pm\pm}}$. As a result, the main contribution to the mass eigenstate

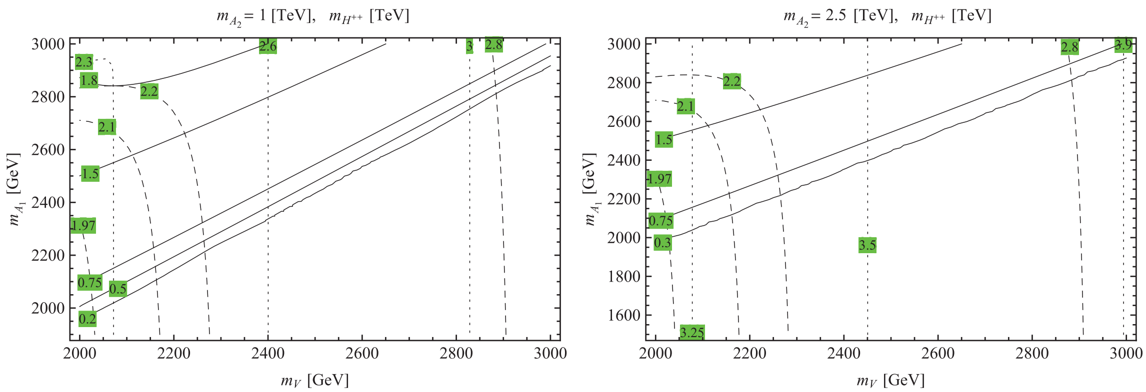

Fig. 2. Contour plots for the masses of DCHs as functions of m_{A_1} and m_V. The left (right) panel corresponds to $m_{A_2} = 1$ (2.5) TeV. The heaviest DCH is represented by dotted curves, the second heaviest by dashed curves, and the lightest by solid curves.

of $m^2_{H_1^{\pm\pm}}$ is $H_1'^{\pm\pm} = -c_\beta \chi^{\pm\pm} + s_\beta \chi'^{\pm\pm}$, i.e., $\Lambda_{1i}, \Lambda_{i1} \simeq \delta_{1i}$ with $i = 1, 2, 3$. This is very useful in finding the coupling formulas between these DCHs with neutral gauge bosons.

The above approximative formulas of DCH masses can precisely predict the constraints of these masses. From Eq. (44), applying Vieta's formulas to the first line of (45), we get a relation

$$m^2_{H_1^{\pm\pm}} + m^2_{H_2^{\pm\pm}} + m^2_{H_3^{\pm\pm}} = m_V^2 + m^2_{A_2} + m^2_{A_1} + m_W^2.$$

Combining this with $m^2_{H_1^{\pm\pm}} = m_V^2 + m^2_{A_2} + \mathcal{O}(m_W^2)$, we have a sum of two DCHs, $m^2_{H_2^{\pm\pm}} + m^2_{H_3^{\pm\pm}} = m^2_{A_1} + \mathcal{O}(m_W^2)$, which is still of the order of the $SU(3)_L$ scale. So there must be at most one light DCH in the model. If the model contains this light Higgs, i.e., $m^2_{H_3^{\pm\pm}} \sim \mathcal{O}(m_W^2)$, we can prove that $m^2_{H_2^{\pm\pm}} \sim m_V^2$. This is the consequence deduced from the last equation of (45) and (46): the condition of the existence of this light Higgs is

$$0 < k_{H^{\pm\pm}} \equiv -c_{2\beta}\left[c_{2\beta} m_V^2 - c_{2\gamma}\left(m_W^2 + m^2_{A_1}\right)\right] \sim \mathcal{O}(m_W^2). \tag{49}$$

This leads to $m^2_{H_2^{\pm\pm}} + m^2_{H_3^{\pm\pm}} \sim \mathcal{O}(m_V^2)$. The mass of the lightest DCH $m^2_{H_3^{\pm\pm}}$ depends directly on the scale of $k_{H^{\pm\pm}}$. It is easy to realize that two mass eigenstates $H^{\pm\pm}_{2,3}$ get their main contributions from $\rho^{\pm\pm}$ and $\rho'^{\pm\pm}$. This is consistent with the fact that the main contribution to the mass of the heavy Higgs $H_2^{\pm\pm}$ is from the $b_\rho \rho\rho'$ term. The numerical values of these masses are illustrated in Fig. 2.

The condition (49) give a lower bound of $m_{A_1} > 1.8$ TeV. With $m_{A_2} < 3$ TeV, the heaviest DCH is always $H_1^{\pm\pm}$, except in the case of the very light $m_V \simeq 2$ TeV. This explains why $m_{H_1^{\pm\pm}}$ does not depend on m_{A_1}, while it is sensitive to m_V. The second heavy DCH is also independent of small values of m_{A_1}, which can be explained as follows. The condition of avoiding a tachyon DCH (46) implies that $0 < c_{2\beta}/c_{2\gamma} m_V^2 - m_W^2 < m^2_{A_1}$. Therefore, a small m_{A_1} will give $c_{2\beta} m_V^2 - c_{2\gamma} m^2_{A_1} \sim \mathcal{O}(m_W^2)$, which is the condition for the appearance of the very light DCH. This gives

$$\frac{4c_{2\beta} m_V^2 \left(c_{2\beta} m_V^2 - c_{2\gamma} m^2_{A_1}\right)}{m^4_{A_1}} \sim \frac{m_V^2}{m^2_{A_1}} \times \frac{\mathcal{O}(m_W^2)}{m^2_{A_1}} \ll 1,$$

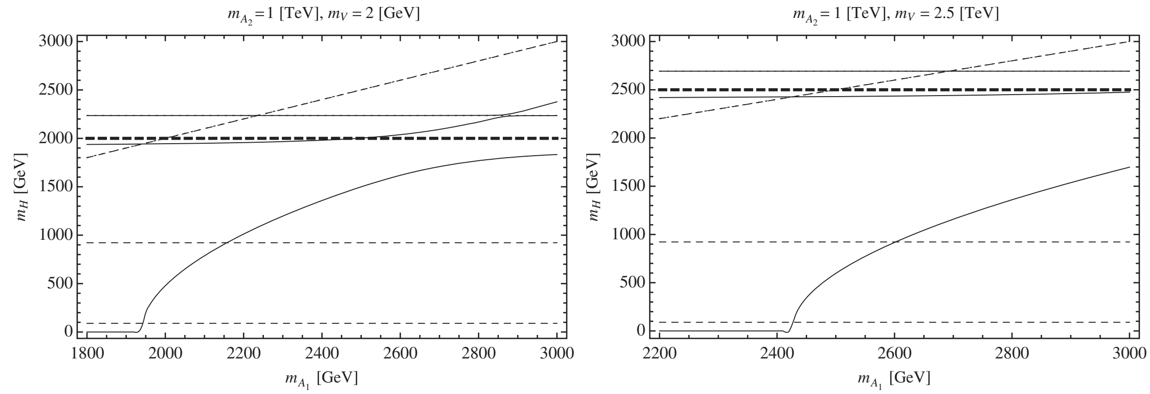

Fig. 3. Plots of mass spectra as functions of m_{A_1} with different fixed m_V. The solid, dotted, dashed, and thick-dashed curves represent DCHs, singly charged, neutral Higgses, and V gauge bosons, respectively.

which we can use for estimating an approximation of $m^2_{H_2^{\pm\pm}}$:

$$m^2_{H_2^{\pm\pm}} \simeq \frac{\left(c_{2\beta}m_V^2 - c_{2\gamma}m^2_{A_1}\right)^2}{m^2_{A_1}} + s^2_{2\gamma}m^2_{A_1} + c_{2\beta}c_{2\gamma}m_V^2.$$

Here, a very small $s^2_{2\gamma}$ is assumed in this work. This means that $m^2_{H_2^{\pm\pm}}$ is sensitive to changes in $c_{2\beta}c_{2\gamma}m_V^2$ but not to small changes in m_{A_1}.

Now we pay attention to the first interesting property relating to the SUSYRM331: it may contain the lightest DCH that does not depend on the SU(3)$_L$ scale but on the specific correlation between m_{A_1} and m_V, as indicated in (49) and illustrated in Fig. 2. It can be seen that there always exists a region of the parameter space containing the mass of this DCH of the order of $\mathcal{O}(100)$ GeV. So the ILC can create this Higgs at a collision energy of 0.5–1.0 TeV, while the two other DCHs are very heavy because of the large lower bound of $m_V \geq 2$ TeV as well as $m_{A_1} > 1.8$ TeV, obtained from condition (49). The lower bound of the first DCH mass is $m_{H_1^{\pm\pm}} \simeq \sqrt{m_V^2 + m^2_{A_2}} = m_{H_2^{\pm}} > 2$ TeV. The additional condition of $m_{A_1} > 1.8$ TeV will result in a larger lower bound of $m_{H_1^{\pm\pm}} > 3$ TeV and be independent of m_{A_2}. The lower bound of $m^2_{H_2^{\pm\pm}}$ directly depends on condition (49), where $m^2_{A_1} > \frac{c_{2\beta}m_V^2}{c_{2\gamma}} - m_W^2$, leading to $m_{H_2^{\pm\pm}} > 1.9$ TeV, when $c_{2\beta}, c_{2\gamma} \simeq -1$ are assumed in this work. Hence, the SUSYRM331 model predicts that the DCHs will not appear in e^+e^- colliders with colliding energies below 4 TeV, with the exception of the lightest DCH.

There is a second interesting property of the lightest DCH: it is lighter than all particles including new gauge bosons and singly charged Higgses, as illustrated in Fig. 3. It is easy to see this when we compare all the masses computed above. The exotic quarks as well as their superpartners can be reasonably supposed to be heavier than the lightest DCH; thus, we do not consider them here. Then we can indicate that the lightest DCH decays into only a pair of charged leptons. Recall that all DCHs have a lepton number of two. Therefore, the total lepton number of all the final states of their decays must be the same. In particular, the final states of each decay should contain one bilepton or a pair of charged leptons. From Tables C1 and C2, which list all three- and four-vertex couplings related to DCHs, we can see that, except for the coupling with two leptons, the lightest DCH always couples with at least one heavier particle: another DCH, a singly charged Higgs, a new gauge boson, or a CP-odd neutral Higgs. So, if it exists, the most promising signal of the lightest DCH is the decay into only a pair of leptons. This strongly suggests the possibility of detection of the lightest DCH in e^+e^- colliders such as the ILC or CLIC, even at the low energy of 0.5–1 TeV.

As mentioned above, the state of the lightest DCH is contributed mainly from two Higgses ρ and ρ'. Combining this with the coupling factors between DCHs and charged leptons shown in Table C1, it is easy to prove that the partial decay of this DCH to a pair of same-sign leptons is $\Gamma\left(H^{\pm\pm} \to l_i^{\pm} l_i^{\pm}\right) \sim \left(m_{l_i}/m_W\right)^2$ with $l_i = e,\ \mu,\ \tau$. As a result, we obtain $\text{Br}\left(H^{\pm\pm} \to \tau^{\pm}\tau^{\pm}\right) \simeq 1$, i.e., the number of events of four-tauon signals is equal to that of creating the lightest DCH at e^+e^- colliders.

Because the lightest DCH mainly decays to same-sign τ pairs, the lower bound from experimental searches is 204 GeV [26]. This lightest DCH is very different from other DCHs predicted by other models where they can mainly decay to pairs of two same-sign W bosons or W^-H^- [35–37]. On the other hand, the heavy DCHs predicted by the SUSYRM331 only couple to other bileptons in the model, including $H_2^{\pm}$, $V^{\pm}$, $U^{\pm\pm}$ and their corresponding superpartners. The most interesting coupling is $H_1^{\pm\pm}W^{\mp}H_2^{\mp}$, which was discussed in Refs. [35–37,89] for creating DCHs at LHC through virtual $W^{\pm}$ bosons, while there are no couplings of $H^{\pm\pm}W^{\mp}W^{\mp}$ because of the lepton number conservation. In addition, the masses of the two heavy DCHs are always larger than 1.5 TeV; they do not appear in the e^+e^- colliders such as ILC and CLIC with their recent designs. These two Higgses may only appear at the LHC with high luminosity. In addition, both of them can be created through the channel $pp \to \gamma/Z/Z' \to H^{++}H^{--}$, but only $H_1^{\pm\pm}$ may be created through the channel $pp \to W^{\pm} \to H_1^{\pm\pm}H_2^{\mp}$. Regarding the latter channel, discussions in Refs. [37,89] indicated that it is very hard to find signals of these very heavy DCHs, even at the very high luminosity of 3000 fb^{-1} that LHC can reach. While the former happens for all three DCHs, the two heavy DCHs are also very hard to observe [90].

For the above reason, the SUSYRM331 predicts that only the lightest DCH may be discovered at the LHC and e^+e^- colliders and the signal can be observed through the main channel of $pp/e^+e^- \to \gamma/Z/Z' \to H_3^{++}H_3^{--} \to$ four tauons. With the LHC, one hopes that it will be observed up to mass of 600 GeV with a high luminosity of 3000 fb^{-1}. Because the cross section created is proportional to $1/s^2$, with s being the colliding energy, the signal of DCH at ILC and CLIC seems better than that at LHC. In addition, with the ILC or CLIC, a larger DCH mass range can be observed, so we will mainly pay attention to the lightest DCH at e^+e^- colliders.

Now we will estimate the allowed kinetic condition $2m_{H^{\pm\pm}} \leq E_{\text{cm}}$ for the creation of the lightest DCH at the e^+e^- colliders with a maximal center-of-mass (CM) energy of 3 TeV. Even in the case in which both m_V and m_{A_1} are large, there always exists a region in which the mass of the lightest DCH is of the order of $\mathcal{O}(100)$ GeV. Furthermore, this light value is almost independent of m_{A_2}. Although mass values below 204 GeV for this Higgs were almost excluded recently from its decay into only a pair of tauons [26,27], higher values can be searched for by ILC or CLIC with a CM energy of about 1 TeV.

The appearance of the light DCH may give large loop corrections to the decays of well known particles. The most important is the decay channel of the SM-like Higgs $H_1^0 \to \gamma\gamma$, which gets contributions from only pure loop corrections. The signal strength of this decay is defined as the ratio of the observed cross section and the SM prediction, $\mu_{\gamma\gamma} = \sigma^{\text{obs}}_{H\to\gamma\gamma}/\sigma^{\text{SM}}_{H\to\gamma\gamma}$, and was found to be slightly in excess of 1 [3,4,91,92]. The enhancement is explained by the contributions of new particles to the partial decay width of $H_1^0 \to \gamma\gamma$ [82]. The analytic formula of this decay width is the sum of its three particular parts: SM, SU$(3)_L$ [93], and SUSY contributions. The SM and SUSYRM331 contributions can be deduced based on Refs. [82,94].

The SUSYRM331, with both $SU(3)_L$ and SUSY breaking scales being larger than 7 TeV, results in a consequence that most of the $SU(3)_L$ and SUSY particles give suppressed contributions to this decay, except for the lightest DCH. Hence, $H_1^0 \to \gamma\gamma$ is an important channel to set a lower bound to its mass. We will follow the latest update of $\mu_{\gamma\gamma}$ in Ref. [4], where $\mu_{\gamma\gamma} = 1.12 \pm 0.24$ without any inconsistencies with the ATLAS results. In addition, to simplify the calculation, we consider that the largest new physics effect on the H_1^0 decay is from only the lightest DCH $H_3^{\pm\pm}$ to the partial decay $H_1^0 \to \gamma\gamma$. As a result, we have a very simple formula, which must satisfy the experimental constraint: $0.88 = 1.12 - 0.24 \leq \mu_{\gamma\gamma}^{\mathrm{SUSYRM331}} \leq 1.12 + 0.24 = 1.36$. The partial decay of the $H_1^0 \to \gamma\gamma$ **is** written as

$$\Gamma^{\mathrm{SUSYRM331}}_{H_1^0 \to \gamma\gamma} \simeq \frac{G_\mu \alpha^2 m^3_{H_1^0}}{128\sqrt{2}\pi^3} \left| A^{\mathrm{SM}} + \Delta A \right|^2, \tag{50}$$

where A^{SM} is the contribution from the SM particles, and ΔA is the new contribution from the SUSYRM331 particles. The well known SM formula can be found in many textbooks or publications, e.g., in Ref. [94]. To find a simple analytic formula, our work considers only the case of $c_{2\gamma}, c_{2\beta} \to -1$, where the masses of the DCHs are nearly equal to the diagonal entries of the squared mass matrix (40), being consistent with (48). The lightest DCH mass now satisfies $m^2_{H_3^{\pm\pm}} = \mathcal{O}(100)$ GeV when (49) is satisfied. In addition, the main contribution to the mixing matrix of the DCHs is C_1, shown in (39). Combining this with the discussion on the neutral Higgs sector, we find that the $H_1^0 H_3^{++} H_3^{--}$ coupling is $g_{H^0HH} \simeq \frac{1}{3} g\left(t^2+2\right) c_{2\gamma} m_W \simeq -\frac{1}{3} g\left(t^2+2\right) m_W = -\frac{2c_W^2}{3(1-4s_W^2)} m_W$. Following this, the formula of ΔA can be written as [82]

$$\Delta A = -\frac{8c_W^2 m_W^2}{3\left(1-4s_W^2\right) m^2_{H_3^{\pm\pm}}} A_0(t_H), \tag{51}$$

where $t_H = \frac{m^2_{H_1^0}}{4m^2_{H_3^{\pm\pm}}}$ and

$$A_0(t) = -[t - f(t)]t^{-2},$$
$$f(t) = \begin{cases} \arcsin^2 \sqrt{t} & \text{for } t \leq 1 \\ -\frac{1}{4}\left[\ln\left(\frac{1+\sqrt{1-t^{-1}}}{1-\sqrt{1-t^{-1}}}\right) - i\pi\right]^2 & \text{for } t > 1. \end{cases}$$

The signal strength of the decay $H_1^0 \to \gamma\gamma$ predicted by the SUSYRM331 is shown in Fig. 4, where $m_{H_3^{\pm\pm}} \geq 200$ GeV is allowed, being equal to the lower bound of 200 GeV from the current experiments.

Finally, in order to calculate the cross sections of the DCHs in the e^+e^- colliders, the next subsection will calculate the coupling of $H^{++}H^{--}V^0$.

3.2. *Couplings between DCHs with neutral scalars and gauge bosons*

It is noted that the process $e^+e^- \to H^{++}H^{--}$ through virtual neutral Higgses is involved with the coupling $e^+e^-H^0$. In the SUSY version [12], this kind of coupling is $2gm_e/(m_W c_\gamma)$, while the SUSY version [20] does not have this kind of coupling at the tree level. In this work, we will use

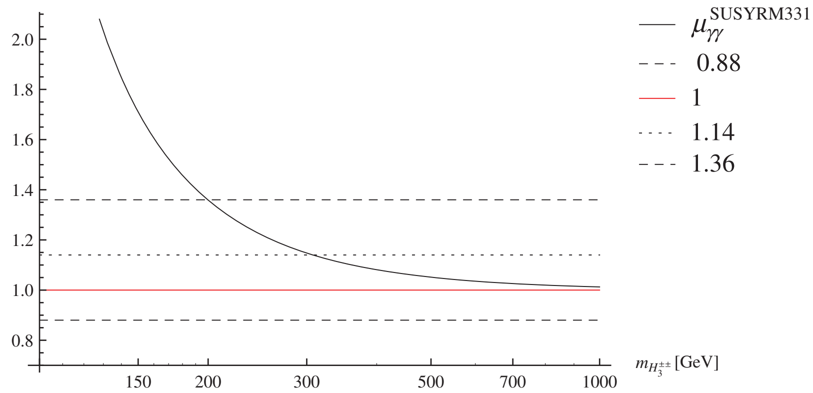

Fig. 4. Signal strength of the decay $H_1^0 \to \gamma\gamma$ as a function of the lightest DCH mass.

the case in Ref. [12]. Corresponding with this, we consider the coupling $H^{++}H^{--}\rho'^0$. Couplings $H^{++}H^{--}H^0$ come from the D-term of the scalar potential (20), namely,

$$\mathcal{L}_{H^{++}H^{--}H^0} = \frac{gm_W}{6}\rho'^0\left(\rho^{--}, \quad \rho'^{--}, \quad \chi^{--}, \quad \chi'^{--}\right) \times \begin{pmatrix} 2s_\gamma\left(t^2-1\right) & -3s_\gamma & 0 & 0 \\ -3c_\gamma & 2c_\gamma\left(t^2+2\right) & 0 & 0 \\ 0 & 0 & 2c_\gamma\left(t^2-2\right) & 0 \\ 0 & 0 & 0 & -2c_\gamma\left(t^2-2\right) \end{pmatrix}\begin{pmatrix} \rho^{++} \\ \rho'^{++} \\ \chi^{++} \\ \chi'^{++} \end{pmatrix}. \quad (52)$$

Because the contributions from neutral Higgs mediations only relate to ρ'^0, the contribution to the $e^+e^- \to H^{++}H^{--}$ amplitude is proportional to

$$\frac{gm_e}{m_W c_\gamma} \times m_W c_\gamma = \frac{m_e e^2}{s^2_{\theta_W}}.$$

This contribution is smaller than that from neutral gauge boson mediation by a factor of $m_e/\sqrt{s}$, so we can neglect it.

The Higgs–Higgs–gauge boson vertices come from the covariant kinetic terms of the Higgses:

$$\begin{aligned}\mathcal{L}_{\mathrm{H}}^{\mathrm{kinetic}} &= \sum_H \left(\mathcal{D}_\mu H\right)^\dagger \mathcal{D}^\mu H, \\ &\to \frac{ig}{2}\left(-\frac{2}{\sqrt{3}}V^{8\mu} + \frac{\sqrt{2}t}{\sqrt{3}}B^\mu\right)\left(\rho^{--}\partial_\mu\rho^{++} + \rho'^{--}\partial_\mu\rho'^{++}\right) \\ &\quad - \frac{ig}{2}\left(-V^{3\mu} + \frac{1}{\sqrt{3}}V^{8\mu} - \frac{\sqrt{2}t}{\sqrt{3}}B^\mu\right)\left(\chi^{--}\partial_\mu\chi^{++} + \chi'^{--}\partial_\mu\chi'^{++}\right) + \mathrm{H.c.}\end{aligned}$$

The interactions among neutral gauge bosons and DCHs can be written as

$$\begin{aligned}\mathcal{L}_{HHV^0} &= i2eA^\mu\left(\rho^{--}\partial_\mu\rho^{++} + \rho'^{--}\partial_\mu\rho'^{++} + \chi^{--}\partial_\mu\chi^{++} + \chi'^{--}\partial_\mu\chi'^{++}\right) \\ &\quad + \frac{ig}{2\sqrt{3}}\left[-\left(c_\zeta + \frac{(2t^2-3)s_\zeta}{\sqrt{2t^2+3}}\right)Z^\mu + \left(s_\zeta - \frac{(2t^2-3)c_\zeta}{\sqrt{2t^2+3}}\right)Z'^\mu\right]\end{aligned}$$

Table 2. Couplings of DCHs with neutral gauge bosons.

$V^\mu H_i^{--} H_i^{++}(p+p')_\mu$	A^μ	Z^μ	Z'^μ
$H_1^{\pm\pm}$	$2ie$	$\frac{ig}{2\sqrt{3}}\left(\frac{2t^2-3}{\sqrt{2t^2+3}}s_\zeta - c_\zeta\right)$	$\frac{ig}{2\sqrt{3}}\left(\frac{2t^2-3}{\sqrt{2t^2+3}}c_\zeta + s_\zeta\right)$
$H_{2,3}^{\pm\pm}$	$2ie$	$\frac{ig}{2\sqrt{3}}\left(\frac{2t^2-3}{\sqrt{2t^2+3}}s_\zeta + c_\zeta\right)$	$\frac{ig}{2\sqrt{3}}\left(\frac{2t^2-3}{\sqrt{2t^2+3}}c_\zeta - s_\zeta\right)$

$$\times \left(\rho^{--}\partial_\mu \rho^{++} + \rho'^{--}\partial_\mu \rho'^{++}\right)$$
$$+ \frac{ig}{2\sqrt{3}}\left[\left(c_\zeta - \frac{(2t^2-3)s_\zeta}{\sqrt{2t^2+3}}\right) Z^\mu - \left(s_\zeta + \frac{(2t^2-3)c_\zeta}{\sqrt{2t^2+3}}\right) Z'^\mu\right]$$
$$\times \left(\chi^{--}\partial_\mu \chi^{++} + \chi'^{--}\partial_\mu \chi'^{++}\right) + \text{H.c.}, \tag{53}$$

where $\mathcal{D}_\mu = \partial_\mu - igV_\mu^a T^a - ig'XT^9 B_\mu$; $T^a = \frac{1}{2}\lambda^a$ or $-\frac{1}{2}\lambda^{a*}$, corresponding to triplet or antitriplet representations of Higgses; and $T^9 = \frac{1}{\sqrt{6}}\text{diag}(1, 1, 1)$. In order to find the couplings of Z, Z' bosons with the DCHs, we have to change the basis $\left(\rho^{--}, \rho'^{--}, \chi^{--}, \chi'^{--}\right)$ into the physical mass states $\left(G^{--}, H_1^{--}, H_2^{--}, H_3^{--}\right)$. Based on (40), if we ignore the suppressed terms containing a factor of m_W^2/m_V^2, we can estimate the $H^{--}H^{++}V^0$ couplings. In the limit $\Lambda_{11} \simeq 1$, $\Lambda_{12} = \Lambda_{13} \to 0$, the couplings of two different DCHs with gauge bosons are very suppressed. So we only investigate the couplings of $H_i^{++}H_i^{--}V$. These couplings are almost independent of Λ_{ij} or the masses of DCHs, as given in Table 2.

4. Signal of doubly charged Higgses in e^+e^- colliders

In an e^+e^- collider, the reaction $e^+e^- \to H^{++}H^{--}$ may involve the mediations of virtual neutral particles such as Higgses and gauge bosons. However, the main contributions relate only to neutral gauge bosons, as shown in the Feynman diagrams in Fig. 5.

In the center-of-mass (CM) frame, the differential cross section for each DCH is given by

$$\frac{d\sigma}{d(\cos\theta)} = \frac{1}{32\pi s}\sqrt{1 - \frac{4m_{H^{\pm\pm}}^2}{s}}\,\overline{|\mathcal{M}|}^2, \tag{54}$$

where $s = (p_1 + p_2)^2 = E_{\text{cm}}^2$ and $\mathcal{M}$ is the scattering amplitude; θ is the angle between $\vec{k}_1$ and $\vec{p}_1$. The detailed calculation is shown in Appendix A. The final result is

$$\frac{d\sigma}{d(\cos\theta)} = -\frac{s}{32\pi}\sqrt{1 - \frac{4m_{H^{\pm\pm}}^2}{s}} \times \left(|\lambda_L|^2 + |\lambda_R|^2\right)\left(1 + \cos^2\theta\right), \tag{55}$$

where

$$\lambda_L^{H_1} = \sum_a \frac{G_L^a G_H^a}{s - m_V^{a2} + im_V^a\Gamma_a}$$
$$= e^2 \times \left[\frac{2}{s} + \frac{\left(c_\zeta + \frac{3s_\zeta}{\sqrt{2t^2+3}}\right)\left(\frac{2t^2-3}{\sqrt{2t^2+3}}s_\zeta - c_\zeta\right)}{12s_{\theta_W}^2\left(s - m_Z^2 + im_Z\Gamma_Z\right)} + \frac{\left(-s_\zeta + \frac{3c_\zeta}{\sqrt{2t^2+3}}\right)\left(\frac{2t^2-3}{\sqrt{2t^2+3}}c_\zeta + s_\zeta\right)}{12s_{\theta_W}^2\left(s - m_{Z'}^2 + im_{Z'}\Gamma_{Z'}\right)}\right], \tag{56}$$

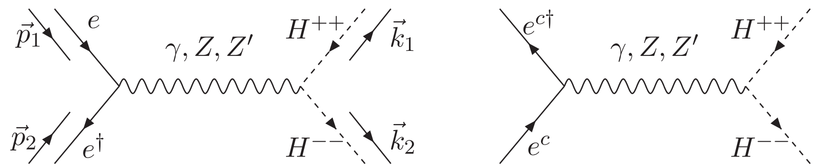

Fig. 5. Feynman diagrams for production of H^{++} and its decays in e^+e^- colliders.

where $a = \gamma, Z, Z'$, the total width of Z' is given in Appendix B, and

$$\lambda_R^{H_1} = \sum_a \frac{G_R^a G_H^a}{s - m_V^{a2} + i m_V^a \Gamma_a}$$
$$= e^2 \left[\frac{2}{s} - \frac{\left(\frac{2t^2-3}{\sqrt{2t^2+3}} s_\zeta - c_\zeta\right)\left(-\frac{3s_\zeta}{\sqrt{2t^2+3}} + c_\zeta\right)}{12 s_{\theta_W}^2 \left(s - m_Z^2 + i m_Z \Gamma_Z\right)} - \frac{\left(\frac{2t^2-3}{\sqrt{2t^2+3}} c_\zeta + s_\zeta\right)\left(\frac{3c_\zeta}{\sqrt{2t^2+3}} + s_\zeta\right)}{12 s_{\theta_W}^2 \left(s - m_{Z'}^2 + i m_{Z'} \Gamma_{Z'}\right)} \right]. \tag{57}$$

Here G_L^a, G_H^a are the couplings of the neutral gauge bosons with two leptons and two DCHs, respectively.

Similarly, in the case of $H_{2,3}^{\pm\pm}$, we have

$$\lambda_L^{H_{2,3}} = e^2 \times \left[\frac{2}{s} + \frac{\left(c_\zeta + \frac{3s_\zeta}{\sqrt{2t^2+3}}\right)\left(\frac{2t^2-3}{\sqrt{2t^2+3}} s_\zeta + c_\zeta\right)}{12 s_{\theta_W}^2 \left(s - m_Z^2 + i m_Z \Gamma_Z\right)} + \frac{\left(\frac{3c_\zeta}{\sqrt{2t^2+3}} - s_\zeta\right)\left(\frac{2t^2-3}{\sqrt{2t^2+3}} c_\zeta - s_\zeta\right)}{12 s_{\theta_W}^2 \left(s - m_{Z'}^2 + i m_{Z'} \Gamma_{Z'}\right)} \right] \tag{58}$$

and

$$\lambda_R^{H_{2,3}} = e^2 \left[\frac{2}{s} - \frac{\left(\frac{2t^2-3}{\sqrt{2t^2+3}} s_\zeta + c_\zeta\right)\left(c_\zeta - \frac{3s_\zeta}{\sqrt{2t^2+3}}\right)}{12 s_{\theta_W}^2 \left(s - m_Z^2 + i m_Z \Gamma_Z\right)} - \frac{\left(\frac{2t^2-3}{\sqrt{2t^2+3}} c_\zeta - s_\zeta\right)\left(\frac{3c_\zeta}{\sqrt{2t^2+3}} + s_\zeta\right)}{12 s_{\theta_W}^2 \left(s - m_{Z'}^2 + i m_{Z'} \Gamma_{Z'}\right)} \right]. \tag{59}$$

The total cross section is

$$\sigma = \frac{s}{12\pi}\sqrt{1 - \frac{4m_{H^{\pm\pm}}^2}{s}} \times \left(|\lambda_L|^2 + |\lambda_R|^2\right). \tag{60}$$

The above process happens only when $\sqrt{s} > 2m_{H^{\pm\pm}} > 400\,\text{GeV}$ from the prediction of the SUSYRM331.

To determine the signals of the lightest DCH, we firstly investigate the dependence of the cross section of the process $e^+e^- \to H_3^{++}H_3^{--}$ on the fixed collision energies of 0.5, 1, 2, and 3 TeV, as shown in Fig. 6. For $\sqrt{s} = 0.5$ TeV, with each fixed value of m_V there exists a very small range of m_{A_1} corresponding to the creation of $H_3^{\pm\pm}$. This is because a small m_{A_1} will create a tachyon DCH while large values will make the masses of the DCHs larger than the allowed kinetic condition. The cross section in this case can reach few pb. For larger $\sqrt{s}$, the cross sections decrease but still reach $\mathcal{O}(0.1)$ pb. One of the most important properties of the lightest SUSYRM331 DCH is that its mass characterizes the difference between two parameters m_{A_1} and m_V. Hence, the signal of DCH requires near-degeneration between these two masses, $|m_{A_1} - m_V| < 100\,\text{GeV}$ when $\sqrt{s} \leq 1$ TeV.

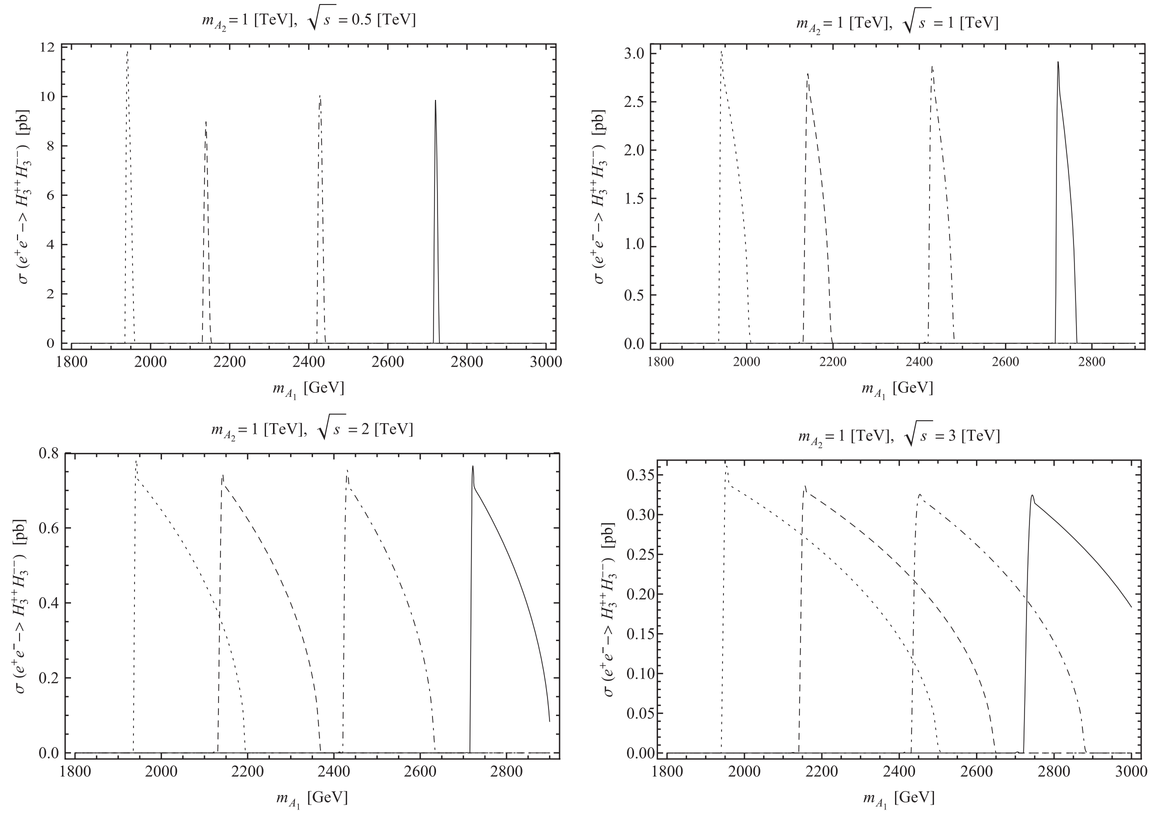

Fig. 6. Plots of the production cross sections of the lightest DCH $H_3^{\pm\pm}$ as a function of m_{A_1} with different colliding energies. The values of m_V are $m_V = 2$, 2.2, 2.5, and 2.8 TeV, represented by dotted, dot-dashed, dashed, and solid curves, respectively.

We can also see that the low colliding energies give a rather large cross section for creating the lightest DCH.

The heavier DCHs may be created with very high collision energies, i.e., higher than 4 TeV. For illustration, Fig. 7 represents the total cross sections $\sigma(e^+e^- \to H^{++}H^{--})$ of three DCHs in a CM energy of $\sqrt{s} = 5$ TeV, although this goes beyond the maximal energy that both ILC and CLIC can reach. Because all $m_{A_1}, m_{A_2}, m_V \gg m_W$, the cross sections of the DCHs depend weakly on the change of m_{A_1}. Apart from $m_{H_{2,3}^{\pm\pm}}$, m_{A_1} only affects the decay width of $m_{Z'}$, which makes a small contribution to the cross section in the limit of very large SUSY and $SU(3)_L$ scales. A value of $m_V = 2$ TeV gives $m_{H_1^{\pm\pm}} \simeq \sqrt{m_{A_2}^2 + m_V^2} = \sqrt{s}$, leading to a rather small cross section of $\mathcal{O}(10^{-2})$ pb (the dotted curve in the left-hand panel), and does not depend on m_{A_1}, while the value of $m_V = 2.5$ TeV gives $m_{H_1^{\pm\pm}} > \sqrt{s}$, and $H_1^{\pm\pm}$ cannot appear. For $H_2^{\pm\pm}$, as explained above, its mass is also independent of small m_{A_1}. Furthermore, all couplings and gauge boson masses related to the cross sections are independent of the mentioned range of m_{A_1}. So the $\lambda^H_{L,R}$ shown in (56)–(59) will become constant too, giving the same property of the cross section for this DCH. However, it is very sensitive to m_V. In particular, it can get a value of 0.1 pb with $m_V = 2$ TeV but this reduces to 0.03 pb for $m_V = 2.5$ TeV. When $\sqrt{s} = 5$ TeV, the cross section of the lightest DCH is 0.1 pb for all masses satisfying the kinetic condition, rather smaller than the other cases with $\sqrt{s} < 3$ TeV.

Figures 6 and 7 only help us see the maximal values of the cross sections for creation of the DCHs. The above discussion does not include the lower bound on the lightest DCH mass. Figure 8 is used to estimate the values of the cross sections for $\sqrt{s} = 1$–3 TeV, including both the condition of the

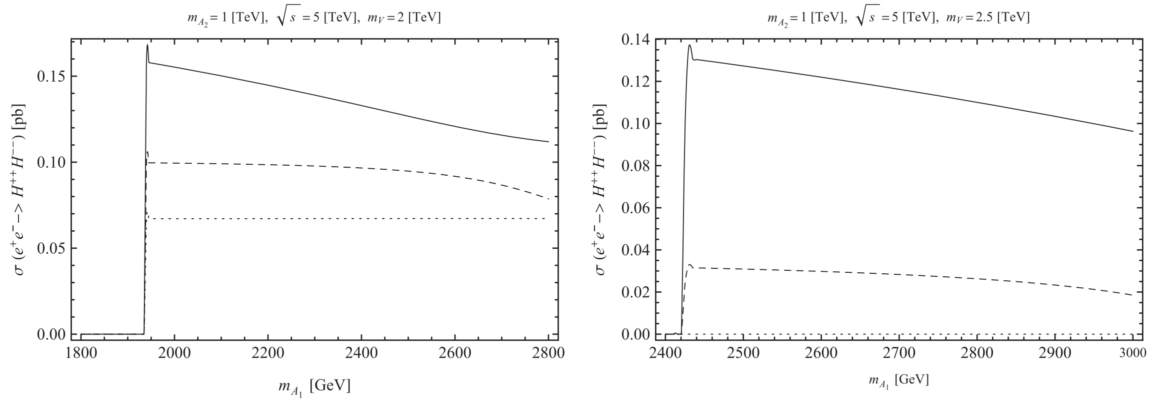

Fig. 7. Total cross sections of creating three DCHs in e^+e^- colliders as a function of m_{A_1} at a very high colliding energy of 5 TeV and $m_V = 2$ (2.5) TeV. The heaviest DCH is represented by dotted curves, the second heaviest by dashed curves, and the lightest by solid curves.

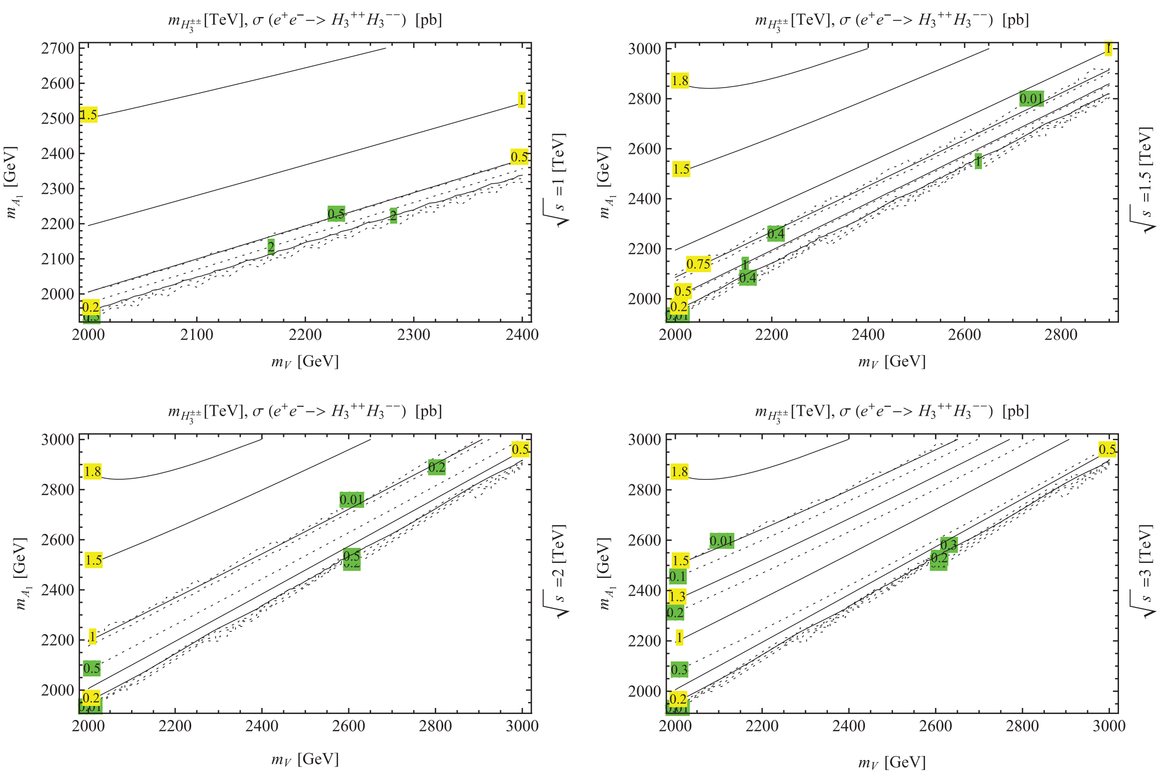

Fig. 8. Contour plots of the mass and the production cross section of the lightest DCH in e^+e^- colliders as functions of m_V and m_{A_1} with different colliding energies of 1, 1.5, 2, and 3 TeV. The mass and the cross section are represented by solid and dotted curves, respectively.

lower DCH mass bound and the allowed kinetic condition for creating heavy physical DCHs. Each panel in the figures has the same interesting properties. When a DCH mass approaches the limit of the kinetic-allowed value, the corresponding cross section will decrease to zero. This explains why the contours of these two quantities almost overlap each other in the limits of $m_{H^{\pm\pm}} \to \sqrt{s}/2$ and cross section $\sigma \to 0$.

In Fig. 8, the cross section can reach a value of a few pb with $\sqrt{s} = 1$ TeV if a lower bound of the DHC mass of 200 GeV is considered. In general, a value of a few pb can be reached by searching for a very light DCH with a mass below 250 GeV in colliding energies in the range of 0.5–1 TeV.

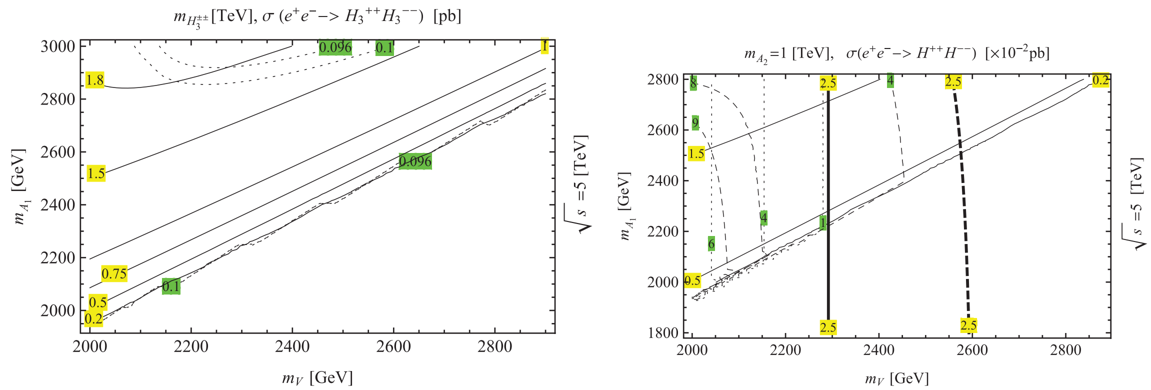

Fig. 9. Contour plots of production cross sections of DCHs in e^+e^- colliders as a function of m_V and m_{A_1} at a colliding energy of 5 TeV. The left panel focuses on the lightest DCH, where the dotted and solid curves describe the cross section and mass, respectively. The right panel represents the cross sections of the remaining two DCHs; the second heaviest and the heaviest are described by dashed and dotted curves, respectively. In addition, the dashed and solid thick curves represent the maximal mass values of the DCHs allowed by the kinetic condition.

These values of the cross section are much smaller than the maximal value for $\sqrt{s} = 0.5$ TeV shown in Fig. 6. In addition, the region of the parameter space allowed for the DCH appearance is very narrow, implying the degeneration of m_{A_1} and m_V. With $\sqrt{s} = 1.5$–2 TeV, the lightest DCH with mass 500 GeV $< m_{H_3^{\pm\pm}} <$ 750 GeV may be detected with the corresponding $\sigma > 0.4$ pb. More interestingly, it can reach 1 pb, twice as large as in the case of $\sqrt{s} = 1$ Tev, if the mass is around 500 GeV. For $\sqrt{s} = 3.0$, the cross sections for $m_{H_3^{\pm\pm}} > 0.5$ TeV are not larger than 0.3 pb. This value is close to the maximal value shown in Fig. 6. From this, we can conclude that the largest cross section for searching for the lightest DCH with a mass from 0.5–0.75 TeV corresponds to intermediate values of $\sqrt{s}$ from 1.5–2 TeV.

Figure 9 shows the rather small cross sections of creating all DCHs when $\sqrt{s} = 5$ TeV. For the lightest, the maximal is below 0.1 pb, while for the two others the value is of the order of 10^{-2} pb.

All the above numerical investigations show that the production cross sections of the lightest DCHs in e^+e^- colliders can be reach values of 10^{-1} to a few pb, depending on the DCH mass and the collision energy. This will be a good signal for the detection of the lightest DCH in near-future colliders [22–25]. In particular, for the ILC, with a collision energy of 0.5–1 TeV, corresponding to an integrated luminosity of 500–1000 fb^{-1} [22,23], the number of events for creation of the lightest DCH will be around 5×10^5–10^6, corresponding to a DCH mass range of 200–500 GeV. With the CLIC [24,25], where the collision energy will increase to 3 TeV or more, the lightest DCH may be observed with a larger mass range. Furthermore, the estimated integrated luminosity targets will be 1.5 ab^{-1} at 1.4 (1.5) TeV and 2 ab^{-1} at 3 TeV collision energy. The DCH with a mass below 750 GeV gives the best signal with $\sqrt{s} = 1.5$–2 TeV, where the observed number of events can reach 6×10^5–1.5×10^6. With $s = 3$ TeV, the maximal number of events reduces to 6×10^5. When the collision energy is high enough to create heavy DCHs, the number of events reduces to 10^4, corresponding to a luminosity of 1 ab^{-1}.

5. Conclusions

We have investigated the Higgs sector of the SUSYRM331 model, where the DCHs are particularly concentrated on as one of the signals indicating new physics at e^+e^- colliders. Here, the masses of neutral CP-even Higgses, DCHs, and the cross sections of the creation of DCHs at e^+e^- colliders can be represented according to five unknown parameters: two masses m_{A_1,A_2} of neutral CP-odd Higgses characterizing the soft scale; the mass of the singly charged heavy gauge boson m_V–SU(3)$_L$ breaking scale; and both γ and β, relating to the ratios of the VEVs. This choice of parameters helps us to discuss the relations among not only particle masses but also the breaking scales of the model more easily. We have found the exact condition $\frac{\left(m_{A_1}^2+m_W^2\right)c_{2\gamma}}{m_V^2} < c_{2\beta} < \frac{m_W^2 c_{2\gamma}}{m_V^2+m_{A_2}^2} < 0$ that must be satisfied to avoid tachyons of the DCHs at the tree level. The numerical investigation of the DCHs as a function of m_{A_1} and m_V shows that, even with very large values of m_{A_1}, m_{A_2}, and m_V, there may still exist a light DCH if the value of m_{A_1} is close enough to that of m_V, being consistent with the relation $0 < -c_{2\beta}\left[c_{2\beta}m_V^2 - c_{2\gamma}\left(m_W^2 + m_{A_1}^2\right)\right] \sim \mathcal{O}\left(m_W^2\right)$ found by our analysis. The constraint on the decay $H_1^0 \to \gamma\gamma$ gives a lower bound on the mass of the DCH of about 200 GeV, the same as the experimental value given by CMS. Finally, we have investigated the possibility of creating DCHs in e^+e^- colliders with collision energies from 1 to 3 TeV, and indicated that only the lightest DCH may be created. The production cross sections range from 0.1 to a few pb, depending on the mass range and the collision energy. Because the SUSYRM331 is valid in the limit of the very large SU(3)$_L$ scale, the two other DCHs always have masses above 2 TeV; therefore, they do not appear unless the collision energies are higher than 4 TeV. In any case, they will give small cross sections for all three DCHs, of the order of $\mathcal{O}(10^{-2})$ pb for the two heavier DCHs and 0.1 pb for the lightest. The two heavier DCHs are difficult to observe in the LHC, ILC, and CLIC. On the other hand, the lightest DCH, which only decays to a same-sign pair of charged tauons, gives the most promising signal for searching for it in e^+e^- colliders such as the ILC and CLIC. If it is detected, the numerical investigation in this work will give interesting information on parameters such as m_{A_1} and m_V.

Acknowledgements

This research is funded by the Vietnam National Foundation for Science and Technology Development (NAFOSTED) under grant number 103.01-2014.69.

Funding

Open Access funding: SCOAP^3.

Appendix A. Cross section of $e^+e^- \to H^{++}H^{--}$

The Lagrangian for the process $e^+e^- \to H^{++}H^{--}$ can be written in terms of a two-component spinor:

$$\mathcal{L}_{eeV^0} = -A_\mu^a\left(G_L^a e^\dagger \bar{\sigma}^\mu e - G_R^a e^{c\dagger}\bar{\sigma}^\mu e^c\right) + \sum_{H=H_{1,2,3}^{\pm\pm}} G_H^a A_\mu^a\left(H^{++}\partial_\mu H^{--} - \text{H.c.}\right), \quad \text{(A1)}$$

where $A_\mu^a = A_\mu, Z_\mu, Z'_\mu, G_L^a$, and G_R^a are given in Table 1, and G_H^a is given in Table 2. The Feynman rules can be found in, e.g., Ref. [96]; the details are shown in Fig. A1.

Denoting $k = k_2 - k_1$, the total amplitude for each DCH is written as

$$\begin{aligned} i\mathcal{M}_H &= -i\left(x_2^\dagger[\bar{\sigma}.k]x_1\right)\sum_a \frac{G_L^a G_H^a}{(p_1+p_2)^2 - m_V^{a2}} - i\left(y_2[\sigma.k]y_1^\dagger\right)\sum_a \frac{G_L^a G_H^a}{(p_1+p_2)^2 - m_V^{a2}} \\ &\equiv -i\left(x_2^\dagger[\bar{\sigma}.k]x_1\right)\lambda_L - i\left(y_2[\sigma.k]y_1^\dagger\right)\lambda_R, \end{aligned} \quad \text{(A2)}$$

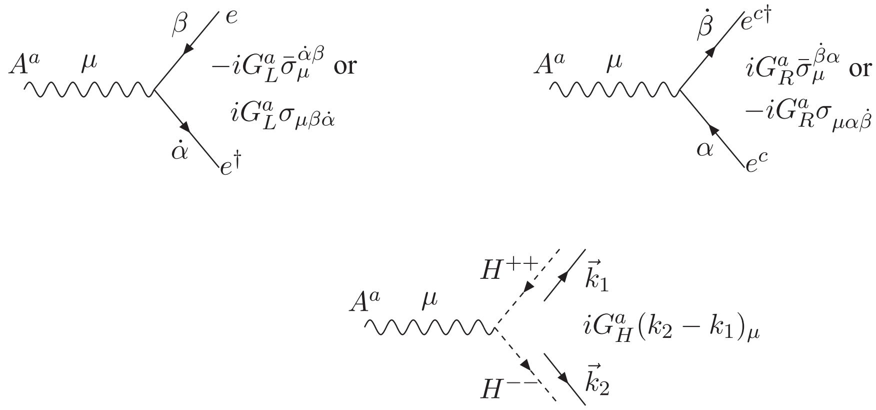

Fig. A1. Feynman rules for interacting vertices of llA^a and $H^{++}H^{--}A^a$, where A^a is a physical neutral gauge boson.

where $m_V^a = 0$ and m_Z, $m_{Z'}$ correspond to photons and Z, Z' bosons. Squaring the amplitude and summing over the electron and positron spins, we have

$$\begin{aligned}\left|\overline{\mathcal{M}}\right|^2 &= \sum_{s_1,s_2} \mathcal{M}_H^\dagger \mathcal{M}_H \\ &= 2\left(|\lambda_L|^2 + |\lambda_R|^2\right)\left[2(p_1.k)(p_2.k) - (p_1.p_2)k^2\right] + 2\Re(\lambda_L^*\lambda_R)m_e^2k^2. \end{aligned} \tag{A3}$$

Now we use the fact that $p_1^2 = p_2^2 = m_e^2 \simeq 0$, $k_1^2 = k_2^2 = m^2_{H^{\pm\pm}}$. Furthermore, all terms in (A3) are invariant under the Lorentz transformation, so the result is unchanged when we use any particular frame. Here we use the center-of-mass frame where the momenta of the two initial particles are

$$p_{1\mu} = (E, 0, 0, E), \quad p_{2\mu} = (E, 0, 0, -E) \tag{A4}$$

with $E = E_{\rm cm}/2 = \sqrt{s}/2$. We define the two four-momenta of the final particles as $k_{1\mu} = (E_1, \vec{k}_1)$ and $k_{2\mu} = (E_2, \vec{k}_2)$. Using the condition of four-momentum conservation, it is easy to prove the following results:

$$\begin{aligned} &k^2 = (k_1 - k_2)^2 = 4m^2_{H^{\pm\pm}} - s, \quad p_1.k = -p_2.k = \frac{s\cos\theta}{2}\sqrt{1 - \frac{4m^2_{H^{\pm\pm}}}{s}} \\ &p_1.p_2 = \frac{s}{2} - m_e^2 \simeq \frac{s}{2}. \end{aligned} \tag{A5}$$

Inserting all results (A5) into (A3), we obtain

$$\begin{aligned}\left|\overline{\mathcal{M}}\right|^2 &= -\left(|\lambda_L|^2 + |\lambda_R|^2\right)s^2\left(1 + \cos^2\theta\right) + 2\Re(\lambda_L^*\lambda_R)m_e^2\left(s - 4m^2_{H^{\pm\pm}}\right) \\ &\simeq -\left(|\lambda_L|^2 + |\lambda_R|^2\right)s^2\left(1 + \cos^2\theta\right). \end{aligned} \tag{A6}$$

Appendix B. Total width of the Z' gauge boson

For any particles ϕ (fermion, gauge boson, scalar) in the model, we define the corresponding covariant derivative related to neutral gauge bosons as $D_\mu\phi \equiv \left(\partial_\mu - iq_\phi A_\mu - ig_Z^\phi Z_\mu - ig_{Z'}^\phi Z'_\mu\right)\phi$. The analytic forms of $g_{Z'}^\phi$ depend on the particular representation of ϕ. In particular, we have

- $SU(3)_L$ singlet

$$g_{Z'}^\phi = \frac{-gY_\phi c_\zeta t^2}{\sqrt{3\left(2t^2 + 3\right)}}$$

Table B1. Couplings of the Z' gauge boson with two gauge bosons (two gauginos).

Gauge boson	$Z'W^+W^-$	$Z'U^{++}U^{--}$	$Z'V^+V^-$
$g^V_{Z'}$, $(g^{\tilde{V}}_{Z'})$	$\frac{g\sqrt{3}}{2}\left(-s_\zeta+\frac{c_\zeta}{\sqrt{2t^2+3}}\right)$	$-\frac{g\sqrt{3}c_\zeta}{\sqrt{2t^2+3}}$	$-\frac{g\sqrt{3}}{2}\left(s_\zeta+\frac{c_\zeta}{\sqrt{2t^2+3}}\right)$

- $\mathrm{SU}(3)_L$ triplet

$$g^\phi_{Z'}=\frac{g}{2\sqrt{3}}\begin{pmatrix} -2\left(s_\zeta+\frac{Y_\phi t^2 c_\zeta}{\sqrt{2t^2+3}}\right) & 0 & 0 \\ 0 & s_\zeta-\frac{c_\zeta\left(2Y_\phi t^2+3\right)}{\sqrt{2t^2+3}} & 0 \\ 0 & 0 & s_\zeta+\frac{c_\zeta\left(-2Y_\phi t^2+3\right)}{\sqrt{2t^2+3}} \end{pmatrix}$$

- $\mathrm{SU}(3)_L$ antitriplet

$$g^\phi_{Z'}=\frac{g}{2\sqrt{3}}\begin{pmatrix} 2\left(s_\zeta-\frac{Y_\phi t^2 c_\zeta}{\sqrt{2t^2+3}}\right) & 0 & 0 \\ 0 & -s_\zeta-\frac{c_\zeta\left(2Y_\phi t^2-3\right)}{\sqrt{2t^2+3}} & 0 \\ 0 & 0 & -s_\zeta-\frac{c_\zeta\left(2Y_\phi t^2+3\right)}{\sqrt{2t^2+3}} \end{pmatrix}$$

- The $\mathrm{SU}(3)_L$ adjoint representation relates to gauge bosons and their superpartners only. The standard couplings of three gauge bosons can be written as $ig^V_{Z'}[g^{\mu\nu}(p-k_1)^\sigma + g^{\sigma\nu}(k_1-k_2)^\mu + g^{\mu\sigma}(k_2-p)^\nu]$, where $g^{VV'}_{Z'}$ is shown in Table B1. With gauginos, the vertices can also be written in the form of $ig^{\tilde{V}}_{Z'}Z'_\mu \tilde{V}^\dagger\bar{\sigma}^\mu\tilde{V}$, where $g^{\tilde{V}}_{Z'}=g^V_{Z'}$.

Below, we will calculate the partial decay width of Z' into three different classes of particles. Analytic formulas can be found in Ref. [95]. For the purpose of estimating the total width decays of Z' as simply as possible, we only consider the largest contribution to each class of particles. In addition, all particles such as gauginos, sleptons, squarks receiving masses from the soft terms are very heavy, so that Z' cannot decay into them. We assume similar situations for cases of exotic quarks. The decay of the Z' related to these particles deserves further detailed study. Here the following numerical values are used: $s_\zeta=0.155$, $c_\zeta=0.988$, corresponding to the definition (8) in the case $m_V\gg m_W$. The value of t follows the definition (9) with $s^2_W=0.231$.

B.1. *Decay of Z' to fermions pairs*

This kind of decay is involved with the Lagrangian below:

$$\mathcal{L}_{Z'ff}=\sum_f Z'^\mu\left(g^f_{Z'}f^\dagger\overline{\sigma}_\mu f+g^{f^c}_{Z'}f^{c\dagger}\overline{\sigma}_\mu f^c\right)=\sum_f Z'^\mu\left(g^f_{Z'}f^\dagger\overline{\sigma}_\mu f-g^{f^c}_{Z'}f^c\sigma_\mu f^{c\dagger}\right), \quad \text{(B7)}$$

Table B2. ZHH couplings.

Vertex	Factor	Vertex	Factor
$Z'H_1^+H_1^-$	$\frac{-ig}{\sqrt{3}}\left(s_\zeta + \frac{t^2 c_\zeta}{\sqrt{2t^2+3}}\right)$	$Z'H_2^+H_2^-$	$\frac{-ig}{\sqrt{3}}\left(s_\zeta - \frac{t^2 c_\zeta}{\sqrt{2t^2+3}}\right)$

where the sum is over all fermions in the model that couple with Z' and satisfy the kinetic condition $m_{Z'} > 2m_f$. Formulas of $g^f_{Z'}$ and $g^{f^c}_{Z'}$ were shown in Table 1. The partial decay width corresponding to each fermion is [96]

$$\Gamma\left(Z' \to ff^+\right) = \frac{N_c^f m_{Z'}}{24\pi}\left(1-\frac{4m_f^2}{m_{Z'}^2}\right)^{1/2}\left[\left(\left|g^f_{Z'}\right|^2+\left|g^{f^c}_{Z'}\right|^2\right)\left(1-\frac{m_f^2}{m_{Z'}^2}\right)-6g^f_{Z'}g^{f^c}_{Z'}\frac{m_f^2}{m_{Z'}^2}\right], \tag{B8}$$

where N_c^f is the color factor, being equal to 3 for quarks and 1 for all other fermions (leptons, quarks, Higgsinos, and gauginos).

B.2. *Decay of Z' to scalar pairs*

The Lagrangian related to these decays is

$$\mathcal{L}_{Z'S_iS_i} = \sum_{S_i,S_j} i g^{S_{ij}}_{Z'} Z'_\mu \left[S_i^\dagger \partial^\mu S_j - (\partial^\mu S_i^\dagger)S_i\right], \tag{B9}$$

where S_i stands for any scalars in the model. The Feynman rule is the same as that for the DCH shown in Fig. A1, where $G^a_H \to i g^{S_{ij}}_{Z'}$. Nonzero values of $g^{S_{ij}}_{Z'}$ for Higgses in the model are shown in Table B2.

If the momentum of the Z' boson is p_μ, then we have $p^2 = m^2_{Z'}$ and $p = k_1 + k_2$. The amplitude of the decay is

$$i\mathcal{M}\left(Z' \to S_iS_j\right) = -g^{S_{ij}}_{Z'}\,(k_2-k_1)\cdot\varepsilon$$

with $\varepsilon_\mu = \varepsilon_\mu(p, \lambda_{Z'})$ being the polarization vector of Z'.

Averaging over the Z' polarization using

$$\frac{1}{3}\sum_{\lambda_{Z'}} \varepsilon_\mu \varepsilon^*_\nu = \frac{1}{3}\left(-g_{\mu\nu} + \frac{p_\mu p_\mu}{m^2_{Z'}}\right), \tag{B10}$$

we obtain the squared amplitude

$$\frac{1}{3}\left|\mathcal{M}\left(Z' \to S_iS_j\right)\right|^2 = \frac{1}{3}\left|g^{S_{ij}}_{Z'}\right|^2\left[-(k_1-k_2)^2 + \frac{\left(k_1^2-k_2^2\right)^2}{m^2_{Z'}}\right]. \tag{B11}$$

Table B3. Coupling of $Z'HV$.

Vertex	Factor	Vertex	Factor
$Z'U^{\pm\pm}\rho^{\mp\mp}$	$\frac{igs_\gamma m_W}{\sqrt{3}}\left(s_\zeta - \frac{2c_\zeta t^2}{\sqrt{2t^2+3}}\right)$	$Z'U^{\pm\pm}\rho'^{\mp\mp}$	$\frac{igc_\gamma m_W}{\sqrt{3}}\left(s_\zeta - \frac{2c_\zeta t^2}{\sqrt{2t^2+3}}\right)$
$Z'U^{\pm\pm}\chi^{\mp\mp}$	$\frac{igs_\beta m_V}{\sqrt{3}}\left(s_\zeta + \frac{2c_\zeta t^2}{\sqrt{2t^2+3}}\right)$	$Z'U^{\pm\pm}\chi'^{\mp\mp}$	$\frac{igm_V c_\beta}{\sqrt{3}}\left(s_\zeta + \frac{2c_\zeta t^2}{\sqrt{2t^2+3}}\right)$
$Z'ZH_\rho$	$\frac{2igc_{2\zeta}s_\gamma\sqrt{2t^2+3}m_V^2 m_W}{3(m_V^2+m_W^2)}$	$Z'ZH_{\rho'}$	$\frac{2igc_{2\zeta}c_\gamma\sqrt{2t^2+3}m_V^2 m_W}{3(m_V^2+m_W^2)}$
$Z'ZH_\chi$	$-\frac{2igc_{2\zeta}s_\beta\sqrt{2t^2+3}m_V m_W^2}{3(m_V^2+m_W^2)}$	$Z'ZH_{\chi'}$	$-\frac{2igc_{2\zeta}c_\beta\sqrt{2t^2+3}m_V m_W^2}{3(m_V^2+m_W^2)}$

Noting that $k_1^2 = m_{S_i}^2$, $k_2^2 = m_{S_j}^2$, and $(k_1-k_2)^2 = 2\left(m_{S_i}^2 + m_{S_j}^2\right) - m_{Z'}^2$ we have the formula of $\Gamma\left(Z' \to SS\right)$, namely,

$$\Gamma(Z' \to S_i S_j) = \frac{1}{16\pi m_{Z'}}\sqrt{\left(1 - \frac{m_{S_i}^2 + m_{S_j}^2}{m_{Z'}^2}\right)^2 - \frac{4m_{S_i}^2 m_{S_j}^2}{m_{Z'}^4}} \times \frac{1}{3}\left|\mathcal{M}\left(Z' \to S_i S_j\right)\right|^2$$
$$= \frac{\left|g_{Z'}^{S_{ij}}\right|^2 m_{Z'}}{48\pi} \times \sqrt{\left(1 - \frac{m_{S_i}^2 + m_{S_j}^2}{m_{Z'}^2}\right)^2 - \frac{4m_{S_i}^2 m_{S_j}^2}{m_{Z'}^4}}$$
$$\times \left[1 - \frac{2(m_{S_i}^2 + m_{S_j}^2)}{m_{Z'}^2} + \frac{\left(m_{S_i}^2 - m_{S_j}^2\right)^2}{m_{Z'}^4}\right] \tag{B12}$$

for two distinguishable final states. For identical final states, there needs to be an extra factor 1/2 to avoid counting each final state twice [97]. Therefore, if $S_i \equiv S_j \to S$, then $m_{S_i} = m_{S_j} = m_S$ and, denoting $g_{Z'}^{S_{ij}} = g_{Z'}^S$, we have a more simple formula:

$$\Gamma\left(Z' \to SS\right) = \frac{|g_{Z'}^S|^2 m_{Z'}}{96\pi}\left[1 - \frac{4m_S^2}{m_{Z'}^2}\right]^{5/2}. \tag{B13}$$

It is noted that $|g_{Z'}^S|^2 \sim g^2/12 \times \mathcal{O}(1)$, as shown in Table 2 for DCHs. This means that

$$\Gamma\left(Z' \to SS\right) \sim \frac{g^2 m_{Z'}}{576\pi} \times \mathcal{O}(1) \ll \Gamma\left(Z' \to ff\right). \tag{B14}$$

B.3. Decay of Z' to one gauge boson and one scalar

This case happens only with scalars that inherit nonzero VEVs, i.e., neutral Higgses in the model. Detailed investigation shows that possible vertices are $Z'H^{++}U^{--}$, $Z'H^{--}U^{++}$, and $Z'ZH^0$. This part of the Lagrangian has the form $g_{Z'}^{SV} Z'_\mu V^\mu S$. Vertex factors are shown in Table B3. The partial decay width for this case is

$$\Gamma(Z' \to SV) = \frac{\left|g_{Z'}^{SV}\right|^2}{48\pi m_{Z'}} \times \sqrt{\left(1 - \frac{m_V^2 + m_S^2}{m_{Z'}^2}\right)^2 - \frac{4m_V^2 m_S^2}{m_{Z'}^4}} \times \left[2 + \frac{\left(m_{Z'}^2 + m_V^2 - m_S^2\right)^2}{4m_V^2 m_{Z'}^2}\right]. \tag{B15}$$

Table C1. Three-vertex coupling of doubly charged Higgses.

Vertex	Factor	Vertex	Factor
$\rho^{++}\rho^{--}Z^{\mu}$	$-\frac{ig}{2\sqrt{3}}\left[\frac{(2t^2-3)s_\zeta}{\sqrt{2t^2+3}}+c_\zeta\right](p+p')_\mu$	$\rho'^{++}\rho'^{--}Z^{\mu}$	$-\frac{ig}{2\sqrt{3}}\left[\frac{(2t^2-3)s_\zeta}{\sqrt{2t^2+3}}+c_\zeta\right](p+p')_\mu$
$\chi^{++}\chi^{--}Z^{\mu}$	$-\frac{ig}{2\sqrt{3}}\left[\frac{(2t^2-3)s_\zeta}{\sqrt{2t^2+3}}-c_\zeta\right](p+p')_\mu$	$\chi'^{++}\chi'^{--}Z^{\mu}$	$-\frac{ig}{2\sqrt{3}}\left[\frac{(2t^2-3)s_\zeta}{\sqrt{2t^2+3}}-c_\zeta\right](p+p')_\mu$
$\rho^{++}U^{--\mu}H_\rho$	$\frac{ig}{2}(p+p')_\mu$	$\rho^{++}U^{--\mu}H_{A_1}$	$\frac{gc_\gamma}{2}(p+p')_\mu$
$\rho^{++}V^{-\mu}H_1^-$	$-\frac{igc_\gamma}{\sqrt{2}}(p+p')_\mu$	$\rho'^{++}U^{--\mu}H_{\rho'}$	$-\frac{ig}{2}(p+p')_\mu$
$\rho'^{++}U^{--\mu}H_{A_1}$	$\frac{-gs_\gamma}{2}(p+p')_\mu$	$\rho'^{++}V^{-\mu}H_1^-$	$\frac{igs_\gamma}{\sqrt{2}}(p+p')_\mu$
$\chi^{++}U^{--\mu}H_\chi$	$-\frac{ig}{2}(p+p')_\mu$	$\chi^{++}U^{--\mu}H_{A_2}$	$\frac{gc_\beta}{2}(p+p')_\mu$
$\chi^{++}W^{-\mu}H_2^-$	$\frac{igc_\beta}{\sqrt{2}}(p+p')_\mu$	$\chi'^{++}U^{--\mu}H_{\chi'}$	$-\frac{ig}{2}(p+p')_\mu$
$\chi'^{++}U^{--\mu}H_{A_2}$	$-\frac{gs_\beta}{2}(p+p')_\mu$	$\chi'^{++}W^{-\mu}H_2^-$	$-\frac{igs_\beta}{\sqrt{2}}(p+p')_\mu$
$\rho'^{--}l_i^c l_i^c$	$\frac{igm_l}{\sqrt{2}m_W c_\gamma c_\beta}$	$\chi'^{++}ll$	$\frac{igm_l}{\sqrt{2}m_V c_\gamma c_\beta}$

We can estimate that the largest contributions to $\Gamma(Z' \to SV)$ are from χ and χ', namely, $\Gamma(Z' \to SV) = 0.06g^2 m_{Z'} \times \mathcal{O}(1)$.

B.4. Decay of Z' to gauge boson pairs

The possible decays are $Z' \to WW, VV, UU$ with the respective couplings shown in Table B1. The general vertex factor is $ig^X_{Z'}[g^{\mu\nu}(p-k_1)^\sigma + g^{\sigma\nu}(k_1-k_2)^\mu + g^{\mu\sigma}(k_2-p)^\nu]$, where $X = W, U$, or V gauge bosons. The partial decay for each particle can be written by

$$\Gamma(Z' \to XX) = \frac{\left|g^X_{Z'}\right|^2 m_{Z'}}{192\pi}\left[1-\frac{4m_X^2}{m_{Z'}^2}\right]^{3/2}\frac{m_{Z'}^4+12m_X^4+20m_X^2 m_{Z'}^2}{m_X^4}. \tag{B16}$$

From the mass spectra of gauge bosons given in Appendix 2.2, we can see that, in the case of $m_W \ll m_V$, we have $m_{Z'}^2 \simeq \frac{2\left(t^2+2\right)}{3}m_U^2$ and $m_U^2 \simeq m_V^2$. Furthermore, from the definition of ζ in (8), we can see that, in the limit of $m_W/m_V \to 0$, we get $g^W_{Z'} \to 0$. More exactly, if $m_W^2/m_V = \epsilon \ll 1$, then $g^W_{Z'} \simeq \frac{\sqrt{3}g\left(t^2+1\right)^2}{\sqrt{2}\left(t^2+2\right)^{3/2}} \times \frac{m_W^2}{m_V^2}$, leading to the result that $\Gamma(Z' \to W^+W^-) \simeq \frac{g^2 m_{Z'}(1+t^2)^2}{648\pi\left(t^2+2\right)}$. It is noted that, in this case, $c_\zeta \simeq 0.988$ and $s_\zeta \simeq 0.155$.

Appendix C. Coupling of doubly charged Higgs

Three-vertex coupling is shown in Table C1, four-vertex coupling in Table C2.

Table C2. Four-vertex coupling of DCHs.

Vertex	Factor	Vertex	Factor
$\rho^{++}\rho^{--}A^{\mu}A_{\mu}$	$4ie^2$	$\rho'^{++}\rho'^{--}A^{\mu}A_{\mu}$	$4ie^2$
$\chi^{++}\chi^{--}A^{\mu}A_{\mu}$	$4ie^2$	$\chi'^{++}\chi'^{--}A^{\mu}A_{\mu}$	$4ie^2$
$\rho^{++}\rho^{--}A^{\mu}Z_{\mu}$	$\frac{-i\sqrt{2}g^2t}{\sqrt{3(2t^2+3)}}\left[\frac{(2t^2-3)s_{\zeta}}{\sqrt{2t^2+3}}+c_{\zeta}\right]$	$\rho'^{++}\rho'^{--}A^{\mu}Z_{\mu}$	$\frac{-i\sqrt{2}g^2t}{\sqrt{3(2t^2+3)}}\left[\frac{(2t^2-3)s_{\zeta}}{\sqrt{2t^2+3}}+c_{\zeta}\right]$
$\chi^{++}\chi^{--}A^{\mu}Z_{\mu}$	$\frac{-i\sqrt{2}g^2t}{\sqrt{3(2t^2+3)}}\left[\frac{(2t^2-3)s_{\zeta}}{\sqrt{2t^2+3}}-c_{\zeta}\right]$	$\chi'^{++}\chi'^{--}A^{\mu}Z_{\mu}$	$\frac{-i\sqrt{2}g^2t}{\sqrt{3(2t^2+3)}}\left[\frac{(2t^2-3)s_{\zeta}}{\sqrt{2t^2+3}}-c_{\zeta}\right]$
$\rho^{++}H_{\rho}U^{--\mu}A_{\mu}$	$\frac{ie^2}{s_W}$	$\rho'^{++}H_{\rho'}U^{--\mu}A_{\mu}$	$\frac{ie^2}{s_W}$
$\chi^{++}H_{\chi}U^{--\mu}A_{\mu}$	$\frac{ie^2}{s_W}$	$\chi'^{++}H_{\chi'}U^{--\mu}A_{\mu}$	$\frac{ie^2}{s_W}$
$\rho^{++}H_{\rho}U^{--\mu}Z_{\mu}$	$-\frac{ig^2}{2\sqrt{3}}\left[\frac{2t^2s_{\zeta}}{\sqrt{2t^2+3}}+c_{\zeta}\right]$	$\rho'^{++}H_{\rho'}U^{--\mu}Z_{\mu}$	$-\frac{ig^2}{2\sqrt{3}}\left[\frac{2t^2s_{\zeta}}{\sqrt{2t^2+3}}+c_{\zeta}\right]$
$\chi^{++}H_{\chi}U^{--\mu}Z_{\mu}$	$\frac{ig^2}{2\sqrt{3}}\left[\frac{2t^2s_{\zeta}}{\sqrt{2t^2+3}}-c_{\zeta}\right]$	$\chi'^{++}H_{\chi'}U^{--\mu}Z_{\mu}$	$\frac{ig^2}{2\sqrt{3}}\left[\frac{2t^2s_{\zeta}}{\sqrt{2t^2+3}}-c_{\zeta}\right]$
$\rho^{++}H_{\rho}V^{-\mu}W^{-}_{\mu}$	$\frac{ig^2}{2\sqrt{2}}$	$\rho'^{++}H_{\rho'}V^{-\mu}W^{-}_{\mu}$	$\frac{ig^2}{2\sqrt{2}}$
$\chi^{++}H_{\chi}V^{-\mu}W^{-}_{\mu}$	$\frac{ig^2}{2\sqrt{2}}$	$\chi'^{++}H_{\chi'}V^{-\mu}W^{-}_{\mu}$	$\frac{ig^2}{2\sqrt{2}}$
$\rho^{++}H_{A_1}U^{--\mu}A_{\mu}$	$\frac{e^2c_{\gamma}}{s_W}$	$\rho'^{++}H_{A_1}U^{--\mu}A_{\mu}$	$\frac{-e^2s_{\gamma}}{s_W}$
$\chi^{++}H_{A_2}U^{--\mu}A_{\mu}$	$\frac{e^2c_{\beta}}{s_W}$	$\chi'^{++}H_{A_2}U^{--\mu}A_{\mu}$	$-\frac{e^2s_{\beta}}{s_W}$
$\rho^{++}H_{A_1}U^{--\mu}Z_{\mu}$	$-\frac{g^2c_{\gamma}}{2\sqrt{3}}\left[\frac{2t^2s_{\zeta}}{\sqrt{2t^2+3}}+c_{\zeta}\right]$	$\rho'^{++}H_{A_1}U^{--\mu}Z_{\mu}$	$\frac{g^2s_{\gamma}}{2\sqrt{3}}\left[\frac{2t^2s_{\zeta}}{\sqrt{2t^2+3}}+c_{\zeta}\right]$
$\chi^{++}H_{A_2}U^{--\mu}Z_{\mu}$	$-\frac{g^2c_{\beta}}{2\sqrt{3}}\left[\frac{2t^2s_{\zeta}}{\sqrt{2t^2+3}}-c_{\zeta}\right]$	$\chi'^{++}H_{A_2}U^{--\mu}Z_{\mu}$	$\frac{g^2s_{\beta}}{2\sqrt{3}}\left[\frac{2t^2s_{\zeta}}{\sqrt{2t^2+3}}-c_{\zeta}\right]$
$\rho^{++}H_{A_1}V^{-\mu}W^{-}_{\mu}$	$\frac{g^2c_{\gamma}}{2\sqrt{2}}$	$\rho'^{++}H_{A_1}V^{-\mu}W^{-}_{\mu}$	$\frac{-g^2s_{\gamma}}{2\sqrt{2}}$
$\chi^{++}H_{A_2}V^{-\mu}W^{-}_{\mu}$	$\frac{-g^2c_{\beta}}{2\sqrt{2}}$	$\chi'^{++}H_{A_2}V^{-\mu}W^{-}_{\mu}$	$\frac{g^2s_{\beta}}{2\sqrt{2}}$
$\rho^{++}H^{-}_{1}V^{-\mu}A_{\mu}$	$\frac{-3ie^2c_{\gamma}}{\sqrt{2}s_W}$	$\rho'^{++}H^{-}_{1}V^{-\mu}A_{\mu}$	$\frac{3ie^2s_{\gamma}}{\sqrt{2}s_W}$
$\chi^{++}H^{-}_{2}W^{-\mu}A_{\mu}$	$\frac{3ie^2c_{\beta}}{\sqrt{2}s_W}$	$\chi'^{++}H^{-}_{2}W^{-\mu}A_{\mu}$	$\frac{-3ie^2s_{\beta}}{\sqrt{2}s_W}$
$\rho^{++}H^{-}_{1}U^{--\mu}W^{+}_{\mu}$	$\frac{-ig^2c_{\gamma}}{2}$	$\rho'^{++}H^{-}_{1}U^{--\mu}W^{+}_{\mu}$	$\frac{ig^2s_{\gamma}}{2}$
$\chi^{++}H^{-}_{2}U^{--\mu}V^{+}_{\mu}$	$\frac{-ig^2c_{\beta}}{2}$	$\chi'^{++}H^{-}_{2}U^{--\mu}V^{+}_{\mu}$	$\frac{ig^2s_{\beta}}{2}$
$\rho^{++}H^{-}_{1}V^{-\mu}Z_{\mu}$	$\frac{ig^2c_{\gamma}}{2\sqrt{6}}\left[\frac{(4t^2-3)s_{\zeta}}{\sqrt{2t^2+3}}-c_{\zeta}\right]$	$\rho'^{++}H^{-}_{1}V^{-\mu}Z_{\mu}$	$-\frac{ig^2s_{\gamma}}{2\sqrt{6}}\left[\frac{(4t^2-3)s_{\zeta}}{\sqrt{2t^2+3}}-c_{\zeta}\right]$
$\chi^{++}H^{-}_{1}W^{-\mu}Z_{\mu}$	$\frac{ig^2c_{\beta}}{2\sqrt{6}}\left[\frac{(4t^2-3)s_{\zeta}}{\sqrt{2t^2+3}}+c_{\zeta}\right]$	$\chi'^{++}H^{-}_{1}W^{-\mu}Z_{\mu}$	$-\frac{ig^2s_{\beta}}{2\sqrt{6}}\left[\frac{(4t^2-3)s_{\zeta}}{\sqrt{2t^2+3}}+c_{\zeta}\right]$

References

[1] ATLAS Collaboration, Phys. Lett. B **716**, 1 (2012) [arXiv:1207.7214 [hep-ex]] [Search INSPIRE].
[2] G. Aad et al. [CMS Collaboration], Phys. Lett. B **716**, 30 (2012) [arXiv:1207.7235 [hep-ex]] [Search INSPIRE].
[3] CMS Collaboration, Eur. Phys. J. C **74**, 3076 (2014).
[4] CMS Collaboration, Eur. Phys. J. C **75**, 212 (2015).
[5] R. N. Mohopatra and J. C. Pati, Phys. Rev. D **11**, 2558 (1975).
[6] G. Senjanovic and R. N. Mohopatra, Phys. Rev. D **12**, 1502 (1975).
[7] G. Senjanovic, Nucl. Phys. B **153**, 334 (1979).
[8] A. Zee, Nucl. Phys. B **264**, 99 (1986).
[9] K. S. Babu, Phys. Lett. B **203**, 132 (1988).
[10] F. Pisano and V. Pleitez, Phys. Rev. D **46**, 410 (1992).
[11] R. Foot, O. F. Hernandez, F. Pisano, and V. Pleitez, Phys. Rev. D **47**, 4158 (1993).
[12] J. G. Ferreira Jr, P. R. D. Pinheiro, C. A. de S. Pires, and P. S. Rodrigues da Silva, Phys. Rev. D **84**, 095019 (2011).
[13] P. H. Frampton, Phys. Rev. Lett. **69**, 2889 (1992).
[14] R. Kuchimanchi and R. N. Mohapatra, Phys. Rev. D **48**, 4352 (1993).
[15] C. S. Aulakh, A. Melfo, and G. Senjanovic, Phys. Rev. D **57**, 4174 (1998).
[16] C. S. Aulakh, A. Melfo, A. Rasin, and G. Senjanovic, Phys. Rev. D **58**, 115007 (1998).
[17] Z. Chacko and R. N. Mohapatra, Phys. Rev. D **58**, 015003 (1998).
[18] K. S. Babu and R. N. Mohapatra, Phys. Lett. B **668**, 404 (2008).
[19] J. C. Montero, V. Pleitez, and M. C. Rodriguez, Phys. Rev. D **65**, 035006 (2002) [arXiv:hep-ph/0012178] [Search INSPIRE].
[20] D. T. Huong, L. T. Hue, M. C. Rodriguez, and H. N. Long, Nucl. Phys. B **870**, 293 (2013).
[21] J. G. Ferreira, C. A. de S. Pires, P. S. Rodrigues da Silva, and A. Sampieri, Phys. Rev. D **88**, 105013 (2013) [arXiv:1308.0575 [hep-ph]] [Search INSPIRE].
[22] T. Behnke et al., [arXiv:1306.6327 [physics.acc-ph]] [Search INSPIRE].
[23] H. Baer et al., [arXiv:1306.6352 [hep-ph]] [Search INSPIRE].
[24] E. Accomando et al. [CLIC Physics Working Group Collaboration], [arXiv:hep-ph/0412251] [Search INSPIRE].
[25] L. Linssen, A. Miyamoto, M. Stanitzki, and H. Weerts, *Physics and Detectors at CLIC: CLIC Conceptual Design Report*, CERN-2012-003, [arXiv:1202.5940 [physics.ins-det]] [Search INSPIRE].
[26] CMS Collaboration, Eur. Phys. J. C **72**, 2189 (2012).
[27] ATLAS Collaboration, Eur. Phys. J. C **72**, 2244 (2012).
[28] ATLAS Collaboration, J. High Energy Phys. **1503**, 041 (2015).
[29] J. Beringer et al. [Particle Data Group], Phys. Rev. D **86**, 010001 (2012).
[30] K. Huitu, J. Maalampi, A. Pietila, and M. Raidal, Nucl. Phys. B **487**, 27 (1997).
[31] J. F. Gunion, Int. J. Mod. Phys. A **11**, 1551 (1996).
[32] K. S. Babu, A. Patra, and S. K. Rai, Phys. Rev. D **88**, 055006 (2013).
[33] J. E. C. Montalvo, N. V. Cortez, and M. D. Tonasse, Phys. Rev. D **78**, 116003 (2008).
[34] J. E. C. Montalvo, G. H. R Ulloa, and M. D. Tonasse, Eur. Phys. J. C **72**, 2210 (2012).
[35] S. Kanemura, M. Kikuchi, H. Yokoya, and K. Yagyu, Prog. Theor. Exp. Phys. **2015**, 051B02 (2015).
[36] S. Kanemura, M. Kikuchi, K. Yagyu, and H. Yokoya, Phys. Rev. D **90**, 115018 (2014).
[37] C. H. Chen and T. Nomura, Phys. Rev. D **91**, 035023 (2015).
[38] D. T. Binh, L. T. Hue, D. T. Huong, and H. N. Long, Eur. Phys. J. C **74**, 2851 (2014) [arXiv:1308.3085 [hep-ph]] [Search INSPIRE].
[39] P. V. Dong, T. D. Tham, and H. T. Hung, Phys. Rev. D **87**, 115003 (2013).
[40] P. V. Dong, D. T. Huong, F. S. Queiroz, and N. T. Thuy, Phys. Rev. D **90**, 075021 (2014).
[41] D. T. Huong, P. V. Dong, C. S. Kim, and N. T. Thuy, Phys. Rev. D **91**, 055023 (2015).
[42] D. T. Huong and H. N. Long, J. Phys. G **38**, 015202 (2011).
[43] D. T. Huong and H. N. Long, Phys. Atom. Nucl. **73**, 791 (2010).
[44] M. Singer, J. W. F. Valle, and J. Schechter, Phys. Rev. D **22**, 738 (1980).
[45] R. Foot, H. N. Long, and T. A. Tran, Phys. Rev. D **50**, R34 (1994) [arXiv:hep-ph/9402243] [Search INSPIRE].
[46] J. C. Montero, F. Pisano, and V. Pleitez, Phys. Rev. D **47**, 2918 (1993).
[47] H. N. Long, Phys. Rev. D **54**, 4691 (1996).

[48] H. N. Long, Phys. Rev. D **53**, 437 (1996).
[49] H. N. Long, Mod. Phys. Lett. A **13**, 1865 (1998) [arXiv:hep-ph/9711204] [Search INSPIRE].
[50] F. Pisano, Mod. Phys. Lett. A **11**, 2639 (1996).
[51] A. Doff and F. Pisano, Mod. Phys. Lett. A **14**, 1133 (1999).
[52] C. A. de S. Pires and O. P. Ravinez, Phys. Rev. D **58**, 035008 (1998).
[53] C. A. de S. Pires, Phys. Rev. D **60**, 075013 (1999).
[54] P. V. Dong and H. N. Long, Int. J. Mod. Phys. A **21**, 6677 (2006).
[55] P. V. Dong, H. N. Long, D. T. Nhung, and D. V. Soa, Phys. Rev. D **73**, 035004 (2006).
[56] P. V. Dong and H. N. Long, Adv. High Energy Phys. **2008**, 739492 (2008).
[57] W. Ponce, Y. Giraldo, and L. A. Sanchez, Phys. Rev. D **67**, 075001 (2003).
[58] V. T. N. Huyen, T. T. Lam, H. N. Long, and V. Q. Phong, [arXiv:1210.5833 [hep-ph]] [Search INSPIRE].
[59] A. G. Dias, R. Martinez, and V. Pleitez, Eur. Phys. J. C **39**, 101 (2005).
[60] A. G. Dias and V. Pleitez, Phys. Rev. D **80**, 056007 (2009).
[61] A. J. Buras, F. D. Fazio, J. Girrbach-Noe, and M. V. Carlucci, J. High Energy Phys. **1402**, 112 (2014).
[62] P. V. Dong and D. T. Si, Phys. Rev. D **90**, 117703 (2014).
[63] M. E. Peskin and T. Takeuchi, Phys. Rev. Lett. **65**, 964 (1990).
[64] M. E. Peskin and T. Takeuchi, Phys. Rev. D **46**, 381 (1992).
[65] M. Drees and K. Hagiwara, Phys. Rev. D **42**, 1709 (1990).
[66] J. C. Montero, C. A. de S. Pires, and V. Pleitez, Phys. Rev. D **66**, 113003 (2002).
[67] C. M. Maekawa and M. C. Rodriguez, J. High Energy Phys. **0604**, 031 (2006).
[68] J. C. Montero, V. Pleitez, and M. C. Rodriguez, Phys. Rev. D **65**, 095008 (2002).
[69] P. V. Dong, D. T. Huong, M. C. Rodriguez, and H. N. Long, Nucl. Phys. B **772**, 150 (2007).
[70] P. V. Dong, Tr.T. Huong, N. T. Thuy, and H. N. Long, J. High Energy Phys. **0711**, 073 (2007).
[71] P. V. Dong, D. T. Huong, N. T. Thuy, and H. N. Long, Nucl. Phys. B **795**, 361 (2008).
[72] D. T. Huong and H. N. Long, J. High Energy Phys. **0807**, 049 (2008).
[73] D. Ng, Phys. Rev. D **49**, 4805 (1994).
[74] D. Cogollo, F. S. Queiroz, and P. Vasconcelos, Mod. Phys. Lett. A **29**, 1450173 (2014).
[75] C. Kelso, P. R. D. Pinheiro, F. S. Queiroz, and W. Shepherd, Eur. Phys. J. C **74**, 2808 (2014) [arXiv:1312.0051 [hep-ph]] [Search INSPIRE].
[76] D. G. Dumm, F. Pisano, and V. Pleitez, Mod. Phys. Lett. A **09**, 1609 (1994).
[77] H. N. Long and V. T. Van, J. Phys. G **25**, 2319 (1999).
[78] A. C. Machado, J. C. Montero, and V. Pleitez, Phys. Rev. D **88**, 113002 (2013).
[79] P. H. Frampton and M. Harada, Phys. Rev. D **58**, 095013 (1998).
[80] H. N. Long and T. Inami, Phys. Rev. D **61**, 075002 (2000).
[81] K. A. Olive et al. [Particle Data Group], Chin. Phys. C **38**, 090001 (2014).
[82] A. Djouadi, Phys. Rept. **459**, 1 (2008).
[83] LHCb Collaboration, Phys. Rev. Lett. **111**, 191801 (2013).
[84] F. Richard, [arXiv:1312.2467 [hep-ph]] [Search INSPIRE].
[85] R. Gauld, F. Goertz, and U. Haisch, J. High Energy Phys. **1401**, 069 (2014).
[86] M. C. Rodriguez, J. Mod. Phys. **2**, 1193 (2011).
[87] L. Girardello and M. T. Grisaru, Nucl. Phys. B **194**, 65 (1982).
[88] R. Barate et al. [LEP Working Group for Higgs boson searches and ALEPH, DELPHI, L3, and OPAL Collaborations], Phys. Lett. B **565**, 61 (2003) [arXiv:hep-ex/0306033] [Search INSPIRE].
[89] B. Dutta, R. Eusebi, Y. Gao, T. Ghosh, and T. Kamon, Phys. Rev. D **90**, 055015 (2014).
[90] G. Bambhaniya, J. Chakrabortty, J. Gluza, M. Kordiaczyńska, and R. Szafron, J. High Energy Phys. **1405**, 033 (2014).
[91] M. Flechl, [arXiv:1503.00632 [hep-ex]] [Search INSPIRE].
[92] ATLAS Collaboration, Phys. Rev. D **90**, 112015 (2014).
[93] W. Caetano, C. A. de S. Pires, P. S. R. da Silva, D. Cogollo, and F. S. Queiroz, Eur. Phys. J. C **73**, 2607 (2013).
[94] A. Djouadi, Phys. Rept. **457**, 1 (2008).
[95] M. Krauß, LHC phenomenology of a Z' decaying into supersymmetric particles, *Master Thesis*, University of Würzburg (2012).
[96] H. K. Dreiner, H. E. Haber, and S. P. Martin, Phys. Rept. **494**, 1 (2010).
[97] S. P. Martin, “Phenomenology of Particle Physics”, NIU Spring 2002 PHYS586 Lecture Notes, the online version: http://www.niu.edu/spmartin/phys686/.